NATIONAL ADVISORY COMMITTEE FOR AERONAUTICS

TECHNICAL NOTE 3481

WIND-TUNNEL INVESTIGATION AT LOW SPEED OF EFFECT OF SIZE AND POSITION OF CLOSED AIR DUCTS ON STATIC LONGITUDINAL AND STATIC LATERAL STABILITY CHARACTERISTICS OF UNSWEPT-MIDWING MODELS HAVING WINGS OF ASPECT RATIO 2, 4, AND 6

By Byron M. Jaquet and James L. Williams

Langley Aeronautical Laboratory
Langley Field, Va.

Washington
September 1955

1F

NATIONAL ADVISORY COMMITTEE FOR AERONAUTICS

TECHNICAL NOTE 3481

WIND-TUNNEL INVESTIGATION AT LOW SPEED OF EFFECT OF SIZE AND POSITION OF CLOSED AIR DUCTS ON STATIC LONGITUDINAL AND STATIC LATERAL STABILITY CHARACTERISTICS OF UNSWEPT-MIDWING MODELS HAVING WINGS OF ASPECT RATIO 2, 4, AND 6

By Byron M. Jaquet and James L. Williams

SUMMARY

An investigation was made at a Mach number of 0.13 in the Langley stability tunnel in order to determine the effects of closed wing-root air ducts (horizontal) on the static longitudinal and static lateral stability characteristics of unswept-midwing models having wings of aspect ratio 2, 4, and 6. In addition, the effects of top and bottom fuselage ducts (vertical) on the static longitudinal and static lateral stability characteristics of model configurations employing the unswept wing of aspect ratio 2 were determined.

The results of the investigation have indicated that, in the low angle-of-attack range, the addition of and increase in size of the horizontal ducts on model configurations employing an unswept wing of aspect ratio 2 resulted in a large forward movement of the aerodynamic center regardless of the vertical location of the horizontal tail. When the aspect ratio of the wing was increased from 2 to 6, this effect became more pronounced. In contrast to this effect of the horizontal ducts, the addition of and increase in size of vertical ducts on model configurations employing the wing of aspect ratio 2 produced a slight rearward movement of the aerodynamic center.

Regardless of the aspect ratio of the wing, the addition of and increase in size of the horizontal ducts caused an increase in directional stability for complete models or a decrease in instability for tail-off configurations at low and moderate angles of attack. The addition of and increase in size of vertical ducts on the models with the wing of aspect ratio 2, however, resulted in large decreases in directional stability which were about constant for the angle-of-attack range investigated.

INTRODUCTION

The stability derivatives of midwing research models which have simple bodies of revolution can, in general, be estimated with good accuracy in the low angle-of-attack range by various theoretical and empirical methods such as those presented in reference 1. When the bodies are changed by the addition of ducts, canopies, or other protuberances, the estimation of the stability derivatives usually becomes more difficult and often impossible as a result of unpredictable interference effects caused by the added items.

Heretofore, data concerning the effects of air ducts on the static longitudinal and static lateral stability characteristics of unswept wing models are virtually nonexistent. The purpose of the present investigation, therefore, was to determine at low speed the effects of size of closed wing-root air ducts (referred to hereinafter as horizontal ducts) on the static longitudinal and static lateral (primarily directional) characteristics of unswept models having wings of aspect ratio 2, 4, and 6. The effect of size of closed top and bottom fuselage air ducts (referred to hereinafter as vertical ducts) on the static longitudinal and static lateral stability characteristics of the unswept model of aspect ratio 2 was also determined. There was no provision made for flow through the ducts.

SYMBOLS

The data presented herein are referred to the stability system of axes shown in figure 1. The moments were measured about 0.25 mean aerodynamic chord for all models. The symbols and coefficients used herein are defined as follows:

L	lift, lb
D	drag, lb
F_Y	lateral force, lb
M_X	rolling moment, ft-lb
M_Y	pitching moment, ft-lb
M_Z	yawing moment, ft-lb

A	aspect ratio, b^2/S
b	span, ft
S	area, sq ft
c	local chord parallel to plane of symmetry, ft
$\bar{c}$	mean aerodynamic chord, $\frac{2}{S}\int_0^{b/2} c^2 dy$, ft
y	spanwise distance measured from and perpendicular to plane of symmetry, ft
q	dynamic pressure, $\frac{\rho V^2}{2}$, lb/sq ft
ρ	mass density of air, slugs/cu ft
V	airspeed, ft/sec
α	angle of attack of fuselage reference line, deg
β	angle of sideslip, deg
C_L	lift coefficient, $\frac{L}{qS_w}$
$C_{L_{max}}$	maximum lift coefficient at first break in curve of C_L against α
C_D	drag coefficient, $\frac{D}{qS_w}$
C_Y	lateral-force coefficient, $\frac{F_Y}{qS_w}$
C_l	rolling-moment coefficient, $\frac{M_X}{qS_w b_w}$
C_m	pitching-moment coefficient, $\frac{M_Y}{qS_w \bar{c}_w}$

C_n yawing-moment coefficient, $\frac{M_Z}{qS_w b_w}$

$C_{m_\alpha} = \frac{\partial C_m}{\partial \alpha}$

$C_{Y_\beta} = \frac{\partial C_Y}{\partial \beta}$

$C_{n_\beta} = \frac{\partial C_n}{\partial \beta}$

$C_{l_\beta} = \frac{\partial C_l}{\partial \beta}$

Subscript:

w wing

The prefix Δ indicates the contribution of the tail assembly to C_{n_β}.

Model Component Designations

For convenience, the model configurations are described by a grouping of the following symbols which denote model components:

F fuselage

W wing (subscripts 2, 4, or 6 indicate aspect ratio of wing)

V vertical tail

H_H high horizontal tail

H_L low horizontal tail

APPARATUS AND MODELS

The 6- by 6-foot curved-flow test section (ref. 2) of the Langley stability tunnel was used for the present investigation. The models were mounted on a single support strut which was rigidly attached to a six-component balance system.

A drawing of the unswept-wing models (wings of aspect ratio 2, 4, and 6) used in the present investigation is presented as figure 2. Additional details of the models are given in table I. Three sizes of ducts, designated 1 (small), 2 (medium), and 3 (large), were tested in the horizontal position (wing-root ducts) on all models and in the vertical position (top and bottom fuselage ducts) only on the models employing the wing of aspect ratio 2. The ratio of maximum duct cross-sectional area (left and right) to maximum fuselage cross-sectional area was 0.246, 0.605, and 1.163 for ducts 1, 2, and 3, respectively. (See table II for duct dimensions.) The ducts were constructed of molded plastic and were not provided with inlets. The inlets were faired out to conform approximately to the streamlines. The end of the fuselage was closed. Photographs of some configurations tested are presented as figure 4. All gaps between the ducts and the wing and fuselage were sealed with plastic tape.

TESTS

The tests to determine the effect of the ducts on the static longitudinal and static lateral characteristics of the models consisted of 6-component measurements through an angle-of-attack range of -4° to 32° (-3° to 33° for models employing the wing of aspect ratio 4) at sideslip angles of 0° and $\pm 5^\circ$. In addition, since a recent investigation in the Langley stability tunnel has indicated aerodynamic hysteresis in sideslip at high angles of attack for the complete model having an unswept wing of aspect ratio 2, a few tests were made at an angle of attack of 24° with this model through a sideslip range of $\pm 10^\circ$ at intervals of 2° to determine the effects of the ducts on the hysteresis.

The test Mach number was 0.13 and the dynamic pressure was 24.9 pounds per square foot. The Reynolds number based on the mean aerodynamic chord of each wing was as follows: for configurations employing the wing of aspect ratio 2, 1.018×10^6; for configurations employing the wing of aspect ratio 4, 0.720×10^6; for configurations employing the wing of aspect ratio 6, 0.586×10^6.

CORRECTIONS

Approximate jet-boundary corrections (ref. 3) were applied to the angle of attack and to the drag coefficient. Horizontal-tail-on pitching-moment coefficients were corrected for the effects of the jet boundaries by the methods of reference 4. The data are not corrected for the effects of the support strut or blockage.

ACCURACY IN DERIVATIVES

The derivative C_{Y_β} is believed to be accurate to within ±0.00035 and since the span varies with aspect ratio the accuracy of C_{l_β} and C_{n_β} also vary as follows:

A_w	Accuracy in C_{l_β} and C_{n_β}
2	±0.00017
4	±.00012
6	±.00010

RESULTS AND DISCUSSION

Presentation of Results

The basic static longitudinal data, which show the effects of the closed wing-root ducts (horizontal) on the variation of C_L, C_D, and C_m with α for various model configurations, are presented in figures 5 to 7. For the model with wings of aspect ratio 2, the effects of horizontal and top and bottom fuselage ducts (vertical) on the variation of C_L, C_D, and C_m with α are shown in figures 8 to 11.

The basic static lateral-stability data, which show the effects of the horizontal ducts on the variation of C_{Y_β}, C_{l_β}, and C_{n_β} with α for various model configurations, are presented in figures 12, 13, and 14. The effects of horizontal and vertical ducts on the variation of C_{Y_β},

C_{l_β}, and C_{n_β} with α are shown in figures 15 to 18 for the model having the wing of aspect ratio 2.

An example of the effect of aerodynamic hysteresis in the variation of C_Y, C_l, and C_n with β at $\alpha = 24.5^\circ$ for several representative model arrangements having the unswept wing of aspect ratio 2 is presented in figures 19, 20, and 21.

The effect of the ducts on the contribution of various tail assemblies to the directional stability of unswept-wing models is shown in figure 22. A summary of the effect of the ducts on $C_{L_{max}}$ and C_{m_α} is presented as figure 23, and a summary of the effect of the ducts on directional stability is presented in figure 24 for $\alpha = 0^\circ$ and in figure 25 for $\alpha = 16^\circ$.

Effect of Horizontal Ducts on Static Longitudinal Characteristics of Unswept Models Having Wings of Aspect Ratio 2, 4, and 6

Lift and drag characteristics.- Regardless of the aspect ratio of the wing or the horizontal-tail location, the addition of and the increase in size of the horizontal ducts has little effect on the variation of C_L with α below the maximum lift coefficient (figs. 5 to 7). For configurations employing the wing of aspect ratio 2, the addition of the small duct increases $C_{L_{max}}$ (fig. 23(b)) and an increase in duct size from the small duct results in a decrease in $C_{L_{max}}$. For configurations employing the wing of aspect ratio 4 the addition of and increase in size of the horizontal ducts generally result in a slight decrease in $C_{L_{max}}$ (fig. 23(c)). The effects of the horizontal ducts on $C_{L_{max}}$ for configurations employing the wing of aspect ratio 6 are very small (fig. 23(d)).

In general, regardless of the wing aspect ratio, the addition of the horizontal ducts and an increase in duct size results in an increase in drag coefficient throughout the angle-of-attack range for each model configuration (figs. 5 to 7). The largest increment in C_D, caused by the addition of the large duct, varied from about 0.018 at $\alpha = 0^\circ$ to 0.124 at $\alpha = 32^\circ$.

Pitching-moment characteristics.- In the low angle-of-attack range, with the horizontal tail high, low, or off, the addition of and increase in

size of the horizontal ducts results in a large forward (destabilizing) movement of the aerodynamic center (figs. 5 to 7) and as the aspect ratio of the wing is increased from 2 to 6 this effect becomes more pronounced (fig. 23). At moderate and high angles of attack there is generally little effect of the ducts on static longitudinal stability but positive increments in pitching-moment coefficients are caused by the addition of and increase in size of the ducts. An analysis of the data of figures 5 to 7 indicates that the ducts have very little effect on the contribution of the horizontal tail to the static longitudinal stability of the models for the angle-of-attack range investigated, and, for $\alpha = 0^\circ$, this effect is shown in figure 23.

Comparison of Effect of Horizontal and Vertical Ducts on Static Longitudinal Characteristics of Model With Wing of Aspect Ratio 2

Lift and drag characteristics.- As in the case of the horizontal ducts, the addition of the ducts in the vertical position on the models employing the wing of aspect ratio 2 has very little effect on the variation of C_L with α below $C_{L_{max}}$ (figs. 8 to 11). Large reductions in $C_{L_{max}}$ are caused by the addition of the vertical ducts, whereas only small reductions were caused by the horizontal ducts (figs. 23(a) and 23(b)).

The effects of the vertical ducts on the drag are similar to the effects of the horizontal ducts at low and moderate angles of attack (figs. 8 to 11). In the high angle-of-attack range, the addition of the vertical ducts generally causes a reduction in the drag coefficient which is probably the result of the large decrease in lift coefficient for the same angle-of-attack range.

Pitching-moment characteristics.- As compared with the horizontal ducts, the addition of the vertical ducts has little effect on static longitudinal stability for the angle-of-attack range investigated (figs. 8 to 11). A slight increase in stability is caused by the addition of the vertical ducts in contrast to the reduction in stability caused by the addition of the horizontal ducts to the models having the wing of aspect ratio 2. This is illustrated for $\alpha = 0^\circ$ in figure 23.

Effect of Horizontal Ducts on Static Lateral Characteristics of Unswept Models Having Wings of Aspect Ratio 2, 4, and 6

Directional stability.- As mentioned previously, some aerodynamic hysteresis in sideslip was encountered with the models employing the wing of aspect ratio 2 and, since this situation results in uncertain derivatives, resort has been made to the use of dashed fairing to distinguish the curves of this region in figure 12 and in figures 15 to 18. Since the slopes are based on a linear interpretation of nonlinear curves, conclusions drawn may not have the proper perspective and, thus, the data in the high angle-of-attack range should be used with care. It is not known if the hysteresis occurs at higher Reynolds numbers. Examples of the effect of the horizontal ducts on the aerodynamic hysteresis in sideslip are presented in figures 19 to 21 for $\alpha = 24.5^\circ$ only. (A more complete study of this phenomenon for this model, with ducts removed, has been made in the Langley stability tunnel.) With the ducts removed, an abrupt change in slope of C_Y, C_n, and C_l with β (figs. 19 to 21) occurs at a positive angle of sideslip when the sideslip angle is varied from negative to positive and when the sideslip angle is varied from positive to negative the converse is true. The addition of horizontal ducts to the wing-fuselage combination or to the complete model in most cases eliminates the hysteresis.

Regardless of the aspect ratio of the wing, the addition of and increase in size of the horizontal ducts causes an increase in directional stability (or decrease in instability for tail-off configurations) at low angles of attack (figs. 12 to 14). Inasmuch as the effect of the ducts on the contribution of the tail assemblies to the directional stability at low angles of attack is small (figs. 22 and 24), it appears that the beneficial increase in directional stability is probably caused by a rearward movement of the lateral center of pressure of the fuselage when the ducts are added. At an angle of attack of 16° (figs 22 and 25), the effects of the ducts on directional stability are similar to the effects at low angles of attack. At higher angles of attack the effects of the ducts on directional stability are generally detrimental (figs. 12 to 14) on the basis of slopes measured between $\beta = \pm 5^\circ$. The contribution of the various tail assemblies to C_{n_β} (fig. 22) is generally increased in the moderate angle-of-attack range and is generally decreased at high angles of attack by the addition of the horizontal ducts. Generally, as the wing aspect ratio is increased from 2 to 6, the effects of the ducts on the tail contribution to C_{n_β} are more favorable in that the tail increments due to the ducts are stabilizing for a greater angle-of-attack range as the wing aspect ratio is increased (fig. 22).

Lateral-force and effective-dihedral parameters.- The effects of the ducts on the lateral-force parameter C_{Y_β} and the effective-dihedral parameter C_{l_β} are generally small and, in some cases are within the accuracy with which the data can be obtained in the low angle-of-attack range (figs. 12 to 14); the derivative C_{Y_β} and the rate of change of C_{l_β} with α generally become more negative as the duct size is increased. At high angles of attack, C_{Y_β} generally becomes considerably more negative and C_{l_β} generally becomes less negative when the ducts are added, although the effects of the ducts are somewhat erratic in this angle-of-attack range.

Comparison of Effect of Horizontal and Vertical Ducts on Static Lateral Characteristics of Model With Wing of Aspect Ratio 2

Directional stability.- In contrast to a small stabilizing effect of the addition of and increase in size of the horizontal ducts, the addition of and increase in size of the vertical ducts on the model with a wing of aspect ratio 2 results in a large decrease in directional stability (increase in instability for wing-fuselage combinations). This can be seen in figures 15 to 18 and in figures 24 and 25. In contrast with the horizontal ducts, the increments in C_{n_β} due to the vertical ducts are more nearly constant with angle of attack. Throughout the angle-of-attack range, the contribution of the various tail assemblies to C_{n_β} is reduced by the addition of the vertical ducts to the model, whereas the addition of the horizontal ducts had little effect on the tail contribution to C_{n_β} at low angles of attack and a stabilizing effect at moderate angles of attack (figs. 22(a) and 22(b)).

It is of interest to note that, with the large vertical duct (duct 3) on the model, directional stability is obtained at $\alpha = 0^\circ$ only when the horizontal tail is in the high position (figs. 15 to 18 and 24). The horizontal tail in this position has a large favorable end-plate effect on the contribution of the vertical tail to C_{n_β}. Also, the increment in C_{n_β} caused by the large duct is equivalent to reducing the vertical-tail area by about two-thirds (fig. 24).

Lateral-force and effective-dihedral parameter.- As would be expected, the addition of and the increase in size of the vertical ducts on the model caused increases in C_{Y_β} for most of the angle-of-attack range, whereas the horizontal ducts had little effect on C_{Y_β} (figs. 15 to 18). The vertical ducts, like the horizontal ducts, had only a small effect on C_{l_β} at low angles of attack, and at high angles of attack the effects of the vertical and horizontal ducts were similar.

CONCLUSIONS

A wind-tunnel investigation at low speed made to determine the effects of size of closed horizontal and vertical air ducts (wing-root and top and bottom fuselage ducts, respectively) on the static longitudinal and static lateral stability characteristics of unswept-midwing models having wings of aspect ratio 2, 4, and 6 has indicated the following conclusions:

1. In the low angle-of-attack range, the addition of and increase in size of horizontal ducts on model configurations employing an unswept wing of aspect ratio 2 resulted in a large forward movement of the aerodynamic center regardless of the vertical location of the horizontal tail. When the aspect ratio of the wing was increased from 2 to 6 this effect became more pronounced. In contrast to this effect of the horizontal ducts, the addition of and increase in size of vertical ducts on model configurations employing the wing of aspect ratio 2 produced a slight rearward movement of the aerodynamic center.

2. Regardless of the aspect ratio of the wing, the addition of and increase in size of the horizontal ducts caused an increase in directional stability of complete models or a decrease in instability for tail-off configurations at low and moderate angles of attack. The addition of and increase in size of the vertical ducts on the models with the wing of aspect ratio 2, however, resulted in large decreases in directional stability which were about constant for the angle-of-attack range investigated.

Langley Aeronautical Laboratory,
National Advisory Committee for Aeronautics,
Langley Field, Va., June 16, 1955.

REFERENCES

1. Campbell, John P., and McKinney, Marion O.: Summary of Methods for Calculating Dynamic Lateral Stability and Response and for Estimating Lateral Stability Derivatives. NACA Rep. 1098, 1952. (Supersedes NACA TN 2409.)

2. Bird, John D., Jaquet, Byron M., and Cowan, John W.: Effect of Fuselage and Tail Surfaces on Low-Speed Yawing Characteristics of a Swept-Wing Model As Determined in Curved-Flow Test Section of the Langley Stability Tunnel. NACA TN 2483, 1951. (Supersedes NACA RM L8G13.)

3. Silverstein, Abe, and White, James A.: Wind-Tunnel Interference With Particular Reference to Off-Center Positions of the Wing and to the Downwash at the Tail. NACA Rep. 547, 1936.

4. Gillis, Clarence L., Polhamus, Edward C., and Gray, Joseph L., Jr.: Charts for Determining Jet-Boundary Corrections for Complete Models in 7- by 10-Foot Closed Rectangular Wind Tunnels. NACA WR L-123, 1945. (Formerly NACA ARR L5G31.)

TABLE I.- DIMENSIONS OF MODEL

Fuselage:			
Length, ft			3.75
Fineness ratio			7.50
Wings:			
Aspect ratio, A_w	2	4	6
Taper ratio, λ_w	0.6	0.6	0.6
Quarter-chord sweep angle, deg	0	0	0
Dihedral angle, deg	0	0	0
Twist, deg	0	0	0
Incidence, deg	0	0	0
NACA airfoil section	65A008	65A008	65A008
Area, S_w, sq ft	2.250	2.250	2.250
Span, b_w, sq ft	2.122	3.000	3.675
Mean aerodynamic chord, $\bar{c}_w$, ft	1.083	0.766	0.625
Root chord, ft	1.326	0.938	0.765
Vertical tail:			
Aspect ratio			2.02
Taper ratio			0.6
Quarter-chord sweep angle, deg			0
NACA airfoil section			65A008
Ratio of tail area to wing area			0.150
Span from fuselage center line, ft			0.825
Tail length, distance measured parallel to fuselage center line from center of gravity to $\bar{c}/4$ of tail, ft			1.392
Mean aerodynamic chord, ft			0.418
Root chord, ft			0.512
Horizontal tail:			
Aspect ratio			4
Taper ratio			0.6
Quarter-chord sweep angle, deg			0
Dihedral angle, deg			0
Twist, deg			0
Incidence, deg			0
NACA airfoil section			65A008
Ratio of tail area to wing area			0.200
Span, ft			1.342
Tail length, distance measured parallel to fuselage center line from center of gravity to $\bar{c}/4$ of tail, ft			1.392
Mean aerodynamic chord, ft			0.343
Root chord, ft			0.419

TABLE II.- DIMENSIONS OF DUCTS IN INCHES

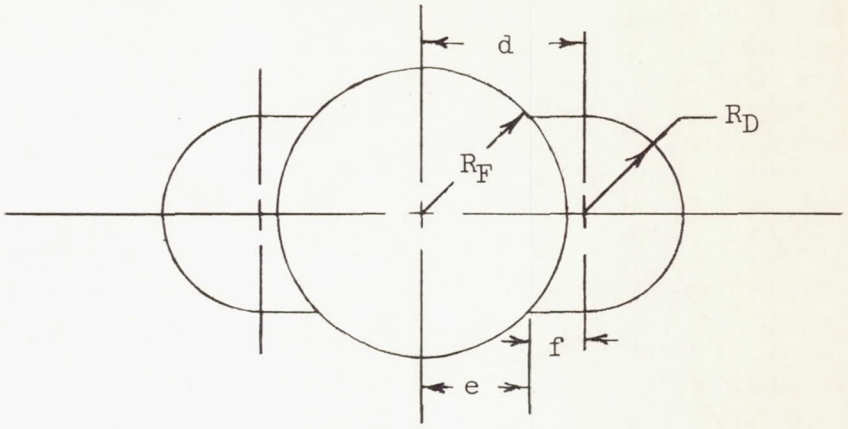

Fuselage station	R_F	d	Duct 1			Duct 2			Duct 3		
			e	f	R_D	e	f	R_D	e	f	R_D
13.50	2.77	2.77	2.77	0	0	2.77	0	0	2.77	0	0
16.00	2.96	3.06	2.89	.17	.64	2.75	.31	1.09	2.54	.52	1.52
18.00	3.00	3.25	2.78	.47	1.13	2.39	.86	1.82	1.66	1.59	2.50
19.00	3.00	3.25	2.73	.52	1.25	2.24	1.01	2.00	1.20	2.05	2.75
22.00	2.97	3.25	2.70	.55	1.25	2.20	1.05	2.00	1.12	2.13	2.75
24.00	2.93	3.25	2.65	.60	1.25	2.14	1.11	2.00	1.02	2.23	2.75
26.00	2.87	3.25	2.61	.64	1.20	2.20	1.05	1.85	1.41	1.84	2.50
28.00	2.79	3.08	2.56	.52	1.12	2.23	.85	1.68	1.67	1.41	2.24
30.00	2.70	2.90	2.51	.39	1.00	2.28	.62	1.45	1.92	.98	1.90
32.00	2.60	2.73	2.48	.25	.77	2.35	.38	1.12	2.15	.58	1.47
34.00	2.47	2.55	2.41	.14	.55	2.34	.21	.80	2.24	.31	1.05
36.00	2.33	2.38	2.32	.06	.30	2.30	.08	.41	2.28	.10	.52
38.25	2.16	2.16	2.16	0	0	2.16	0	0	2.16	0	0

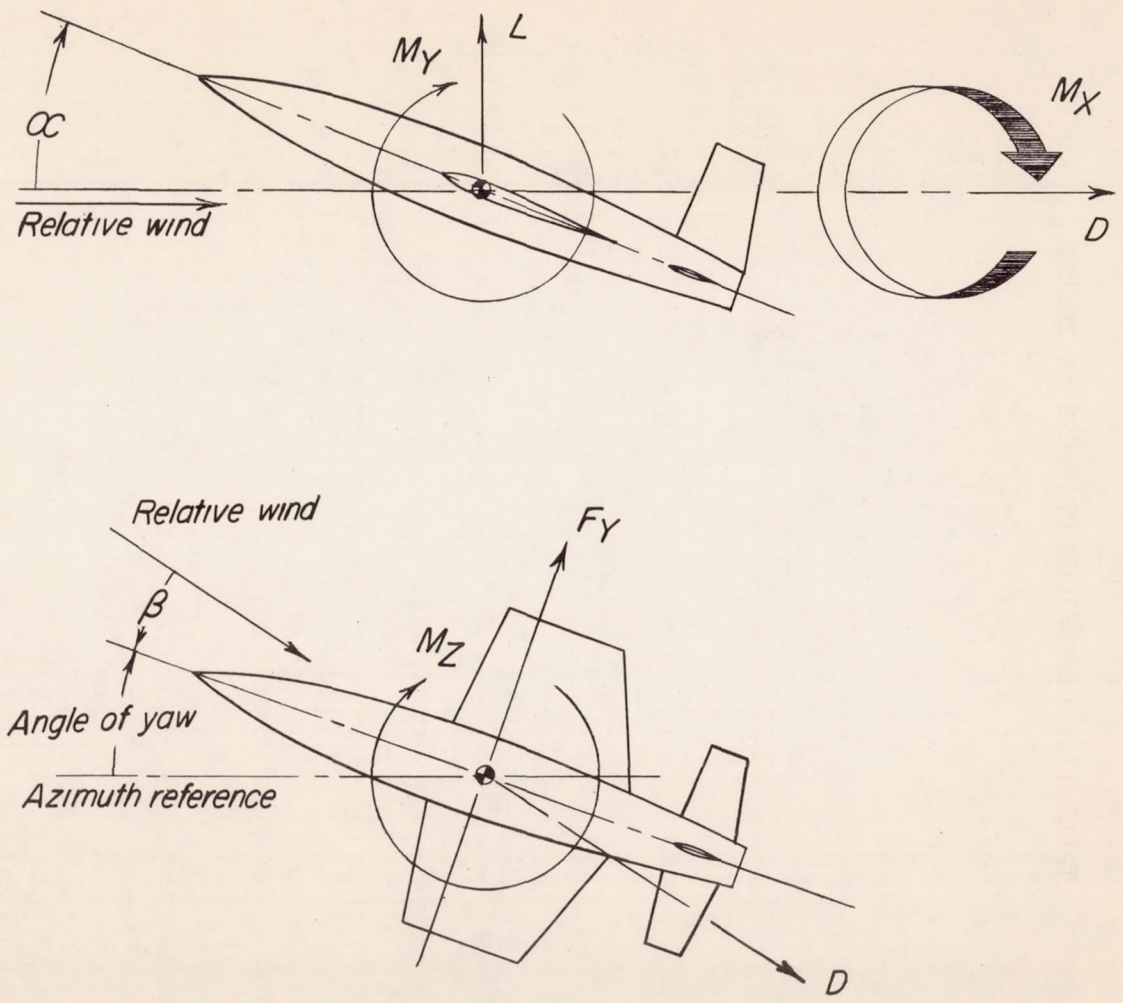

Figure 1.- Stability system of axes. Arrows indicate positive direction of forces, moments, and angular displacements.

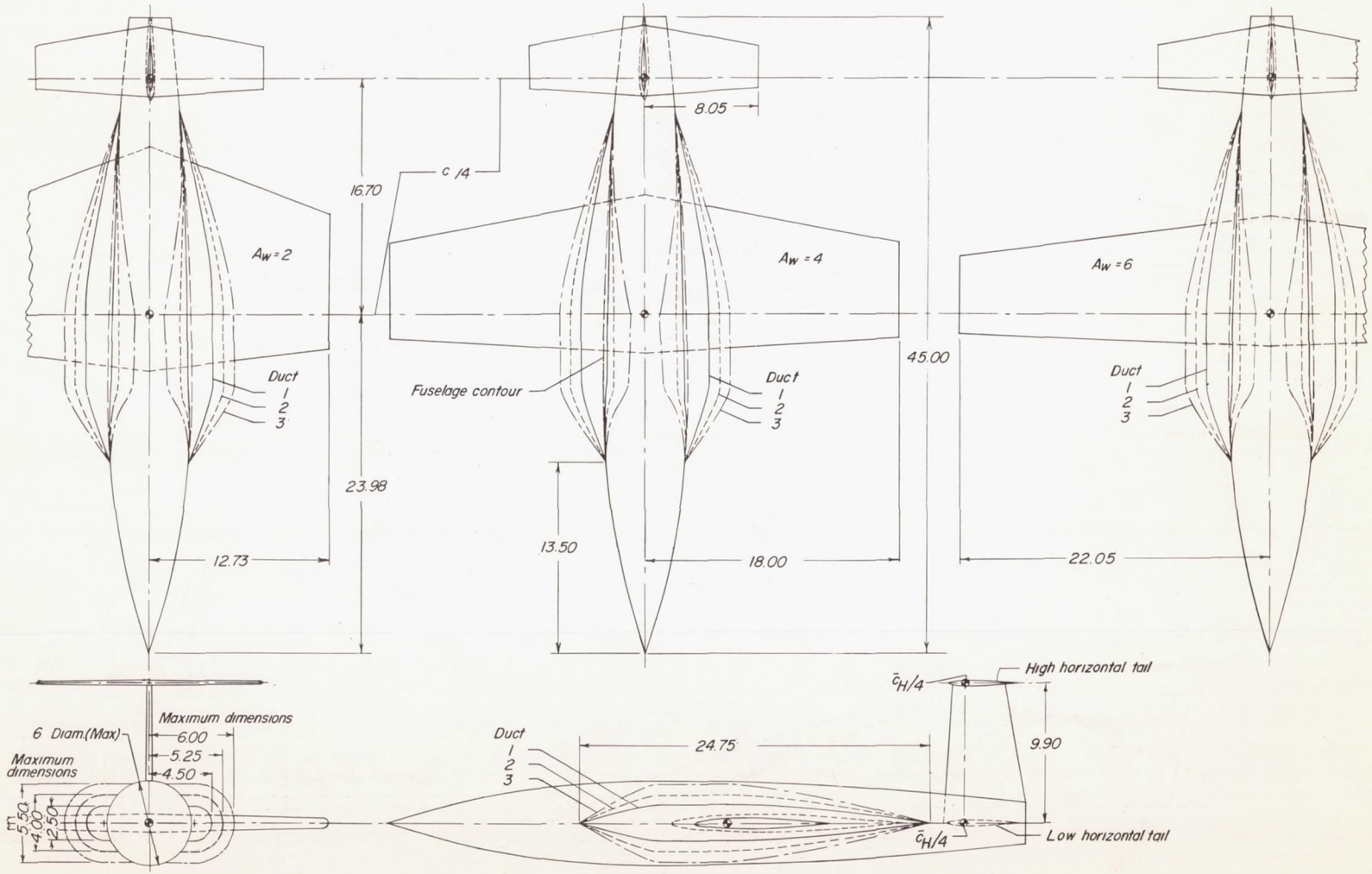

(a) Horizontal ducts.

Figure 2.- General arrangement of models. Dimensions are in inches.

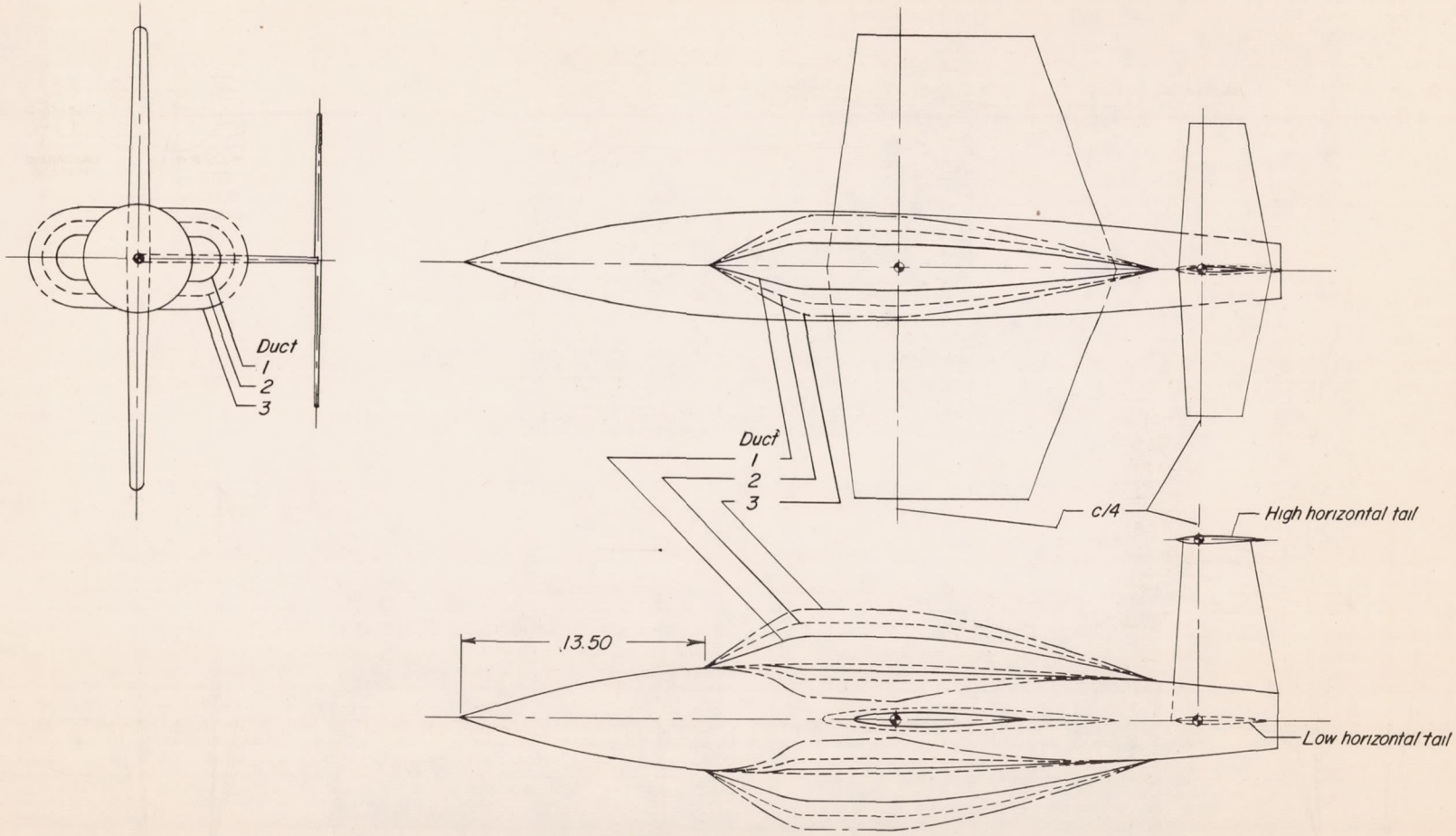

(b) Vertical ducts on model with wing of aspect ratio 2.

Figure 2.- Concluded.

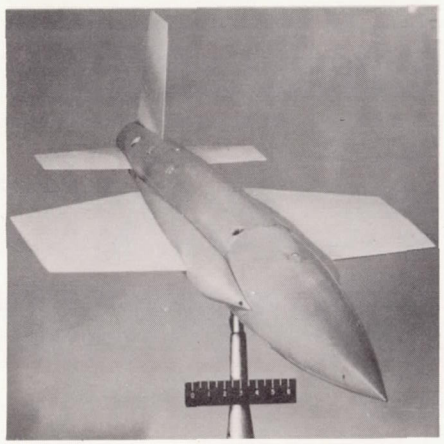

L-82965

(a) Small ducts on configuration FW_2VH_L.

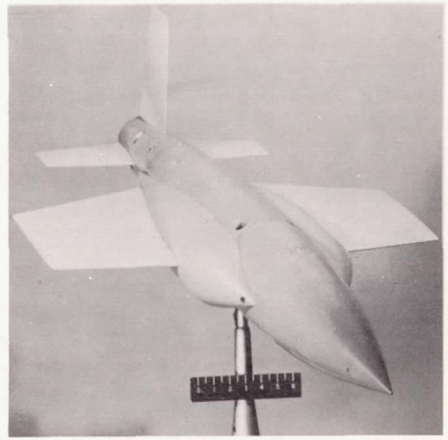

L-82955

(b) Medium ducts on configuration FW_2VH_L.

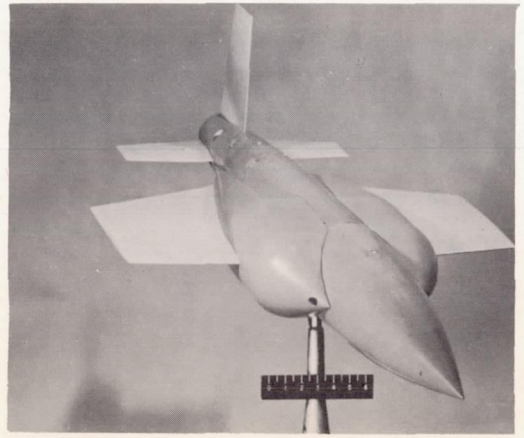

L-82967

(c) Large ducts on configuration FW_2VH_L.

Figure 3.- Photographs of horizontal ducts on model having wing of aspect ratio 2.

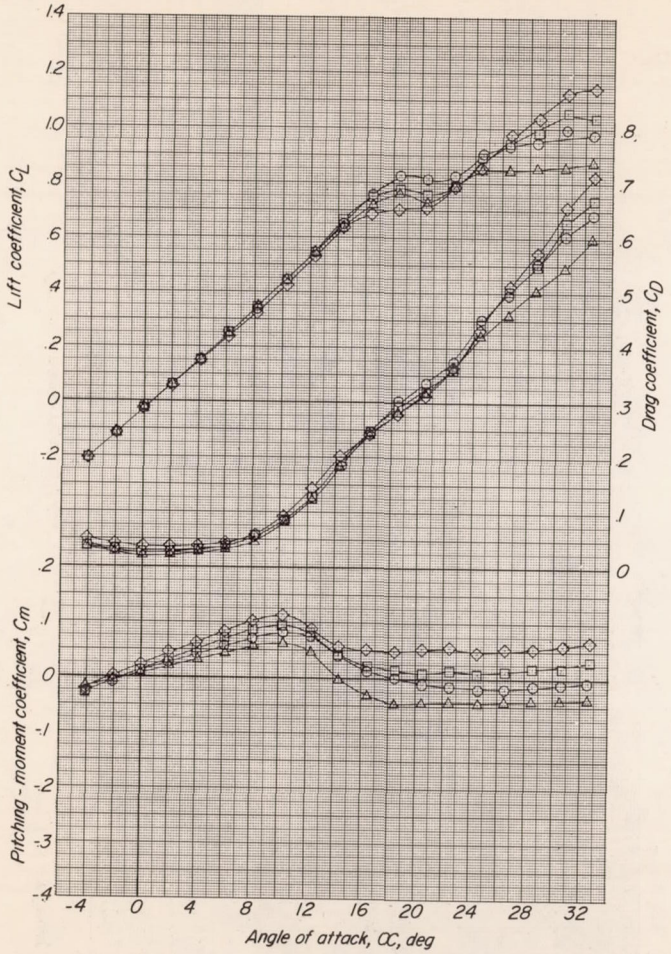

(a) Configuration FW_2.

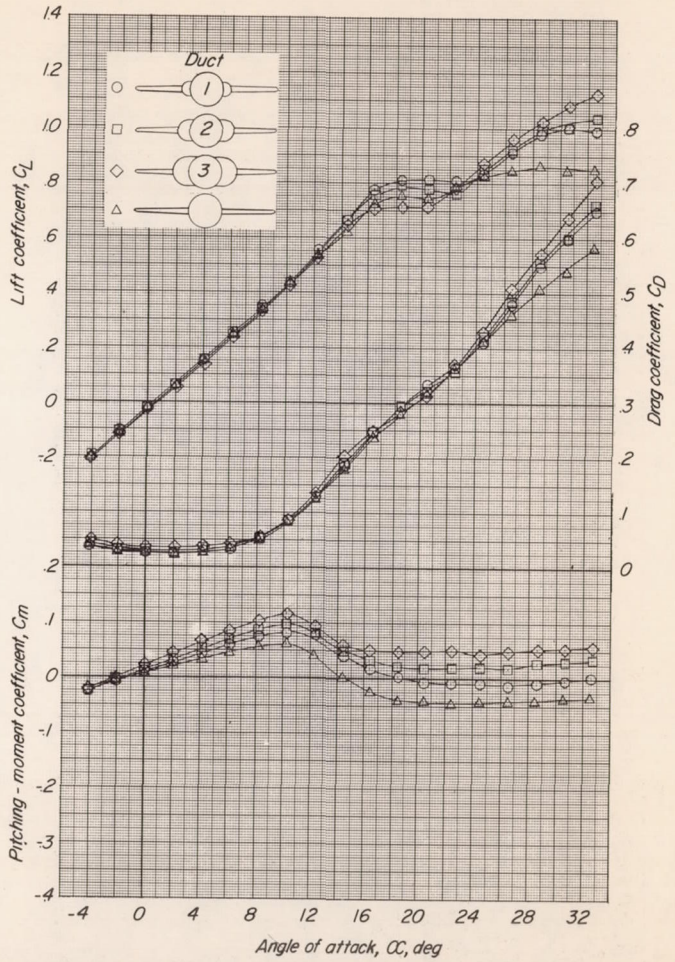

(b) Configuration FW_2V.

Figure 4.- Effect of horizontal air ducts on the variation of C_L, C_D, and C_m with α for model arrangements having an unswept wing of aspect ratio 2.

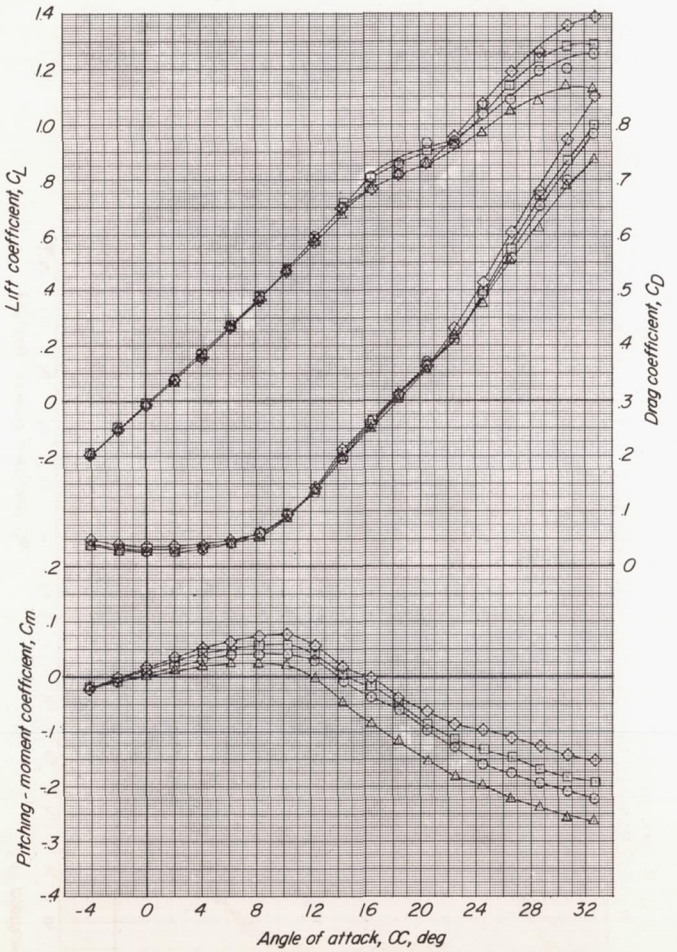

(c) Configuration FW_2VH_L.

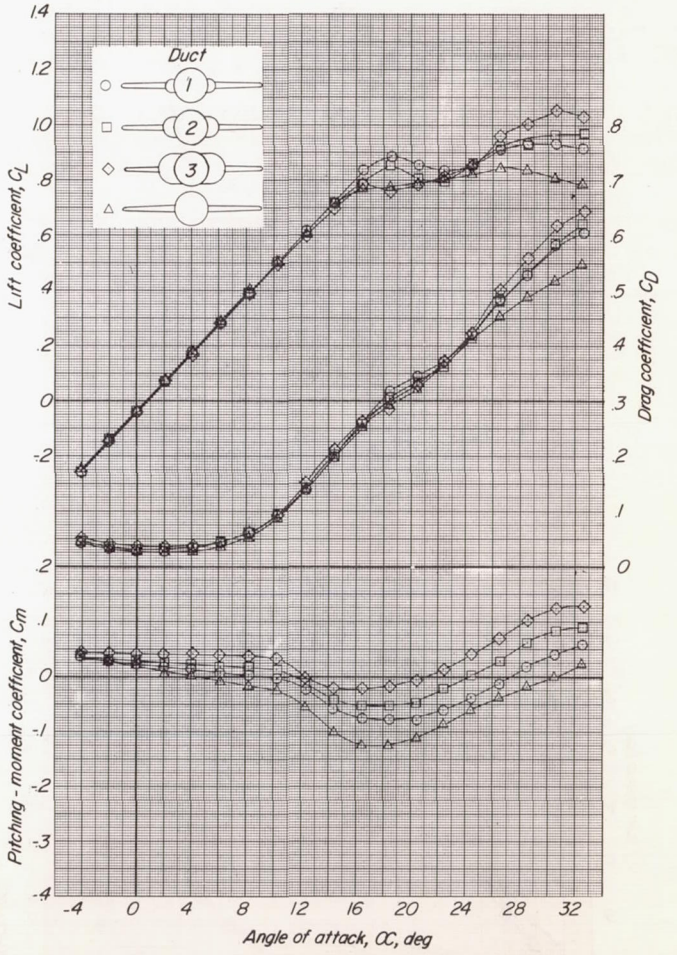

(d) Configuration FW_2VH_H.

Figure 4.- Concluded.

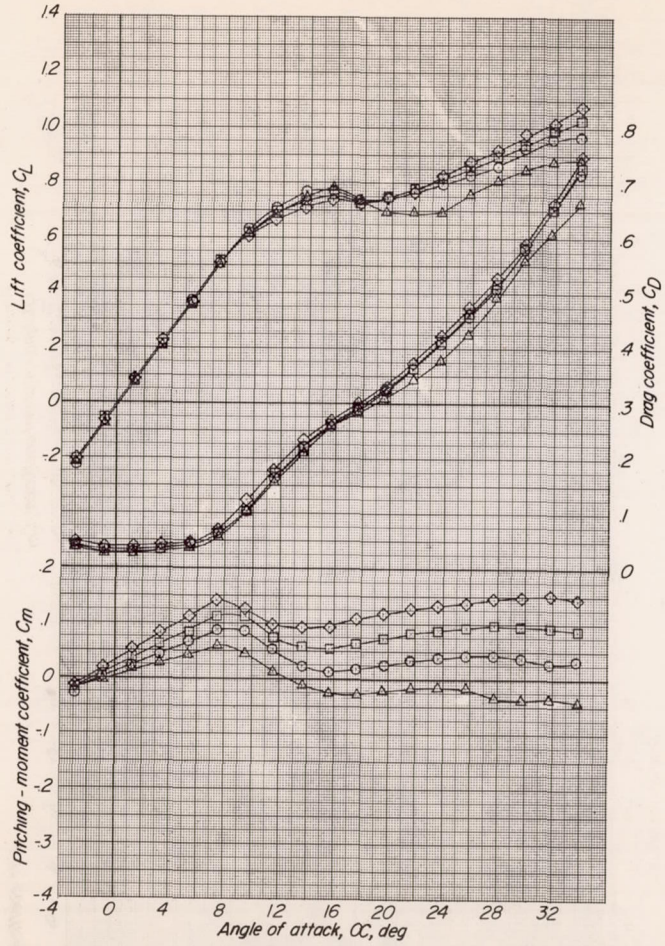

(a) Configuration FW_4.

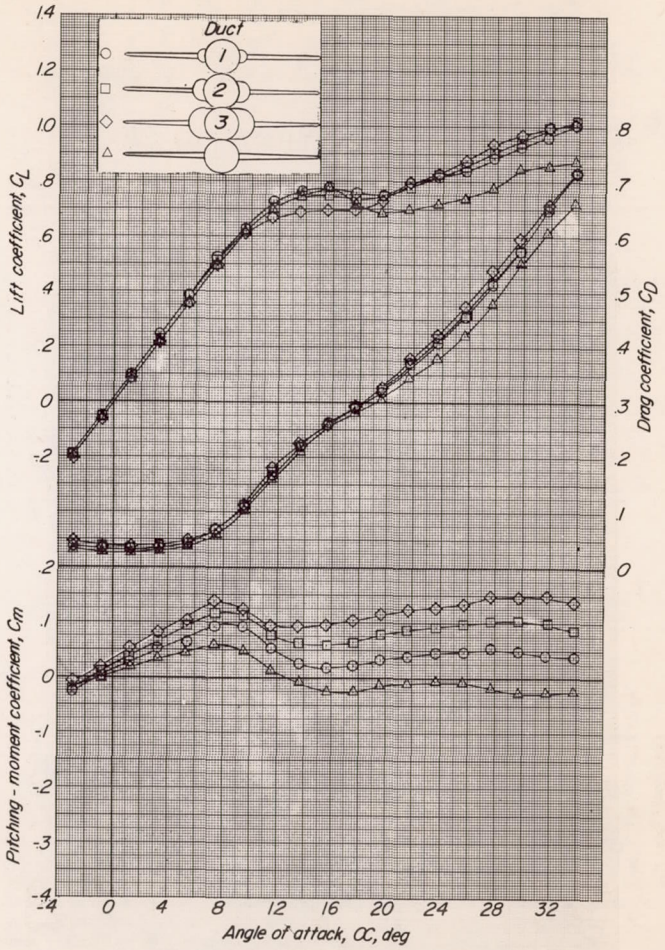

(b) Configuration FW_4V.

Figure 5.- Effect of horizontal air ducts on the variation of C_L, C_D, and C_m with α for model arrangements having an unswept wing of aspect ratio 4.

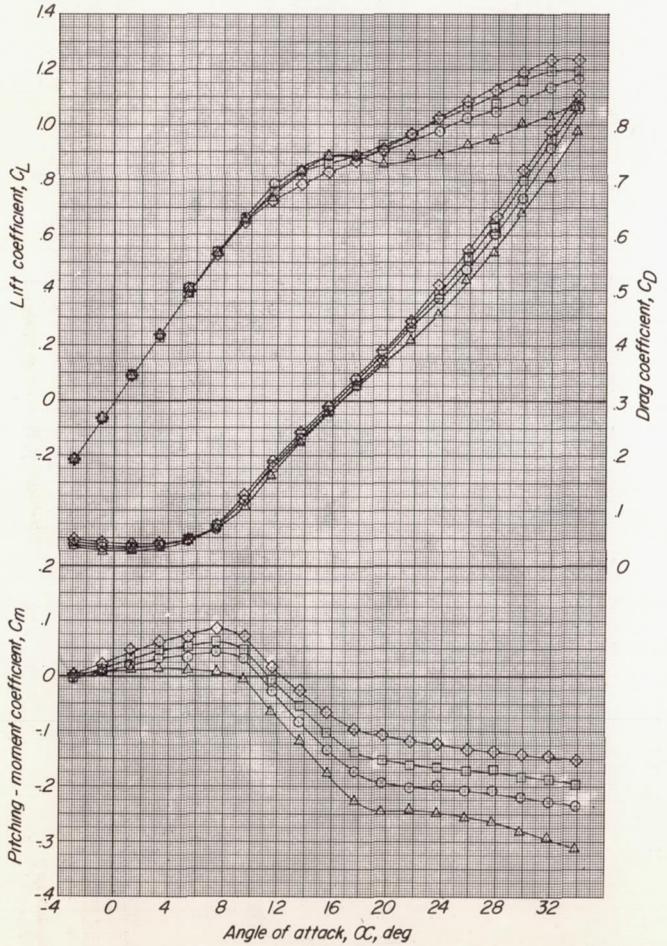

(c) Configuration FW_4VH_L.

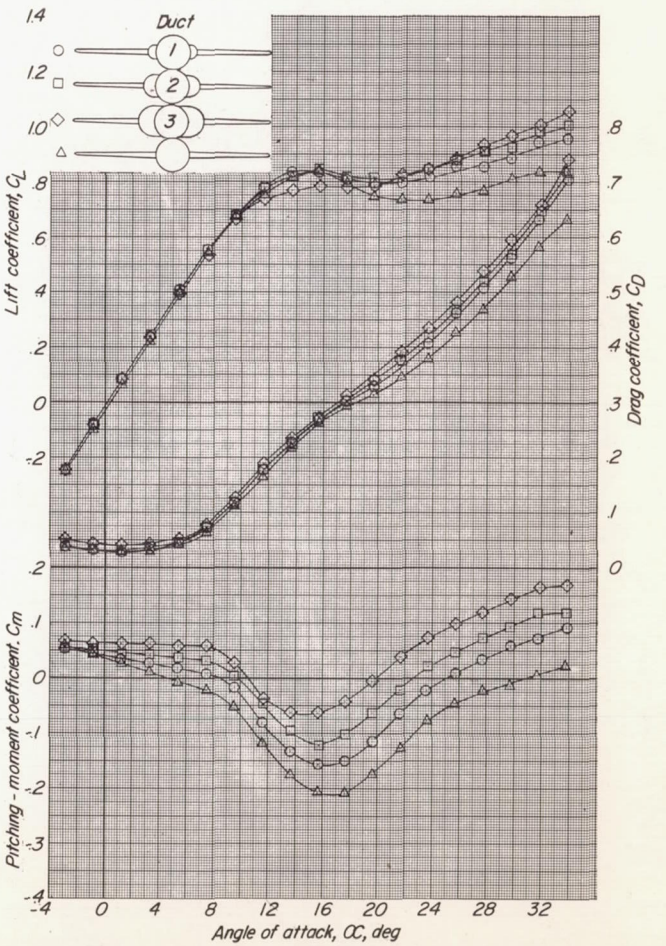

(d) Configuration FW_4VH_H.

Figure 5.- Concluded.

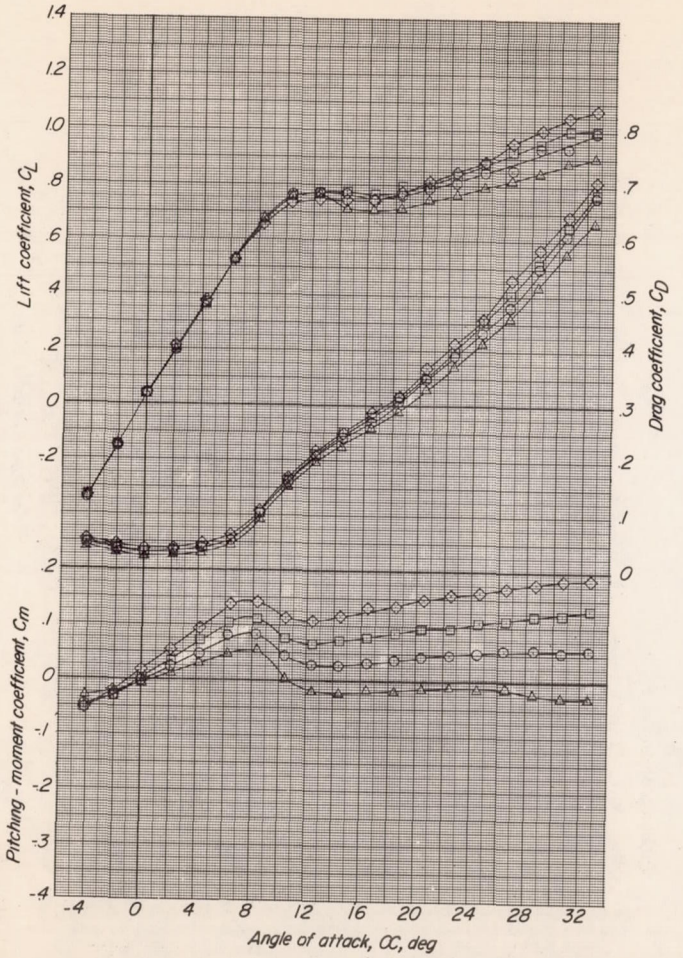

(a) Configuration FW_6.

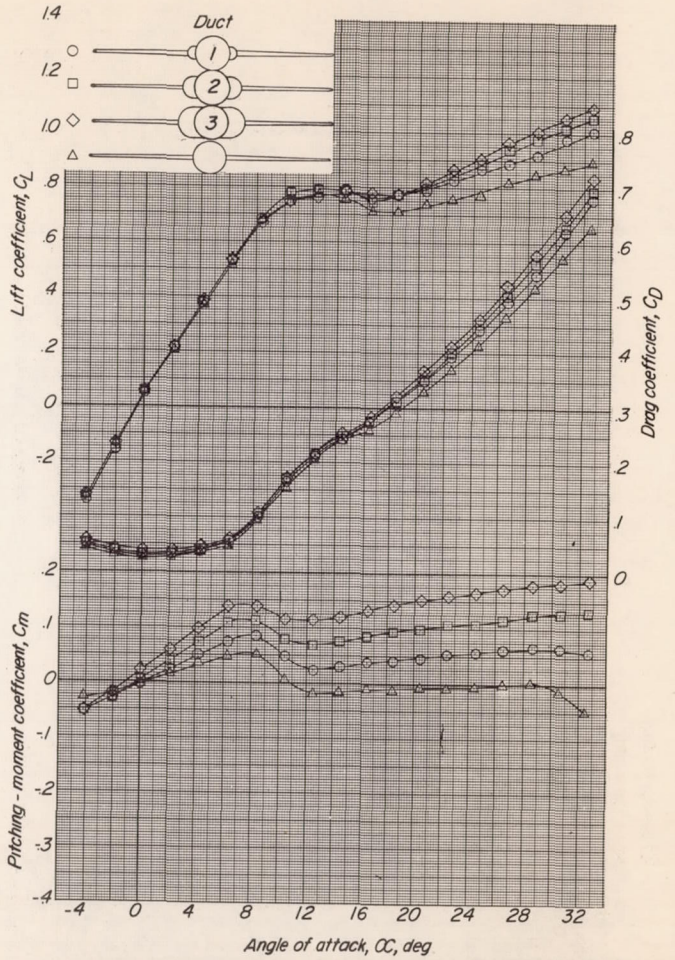

(b) Configuration FW_6V.

Figure 6.- Effect of horizontal air ducts on the variation of C_L, C_D, and C_m with α for model arrangements having an unswept wing of aspect ratio 6.

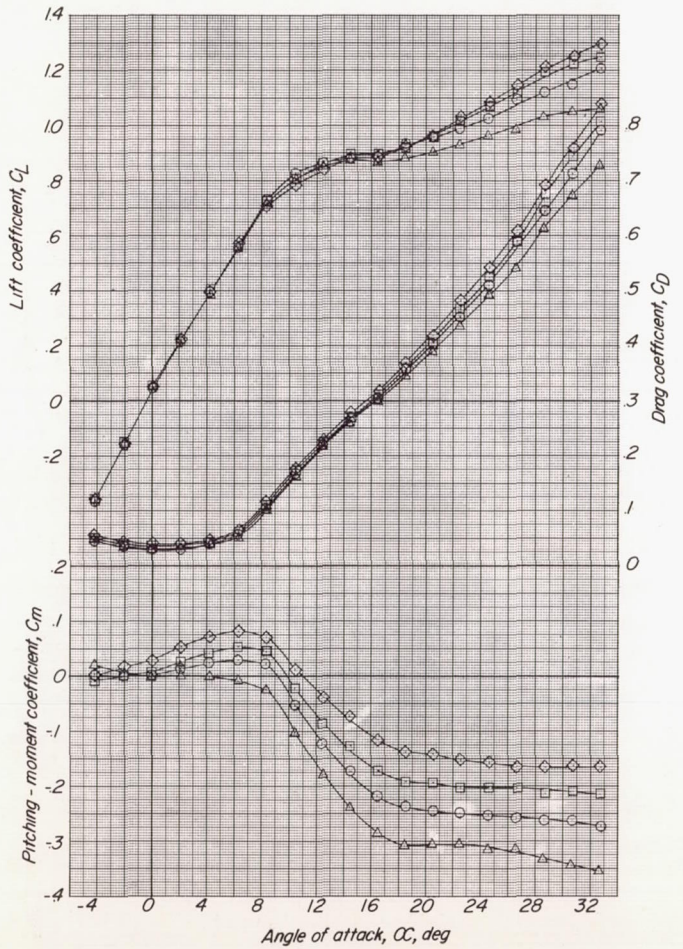

(c) Configuration FW_6VH_L.

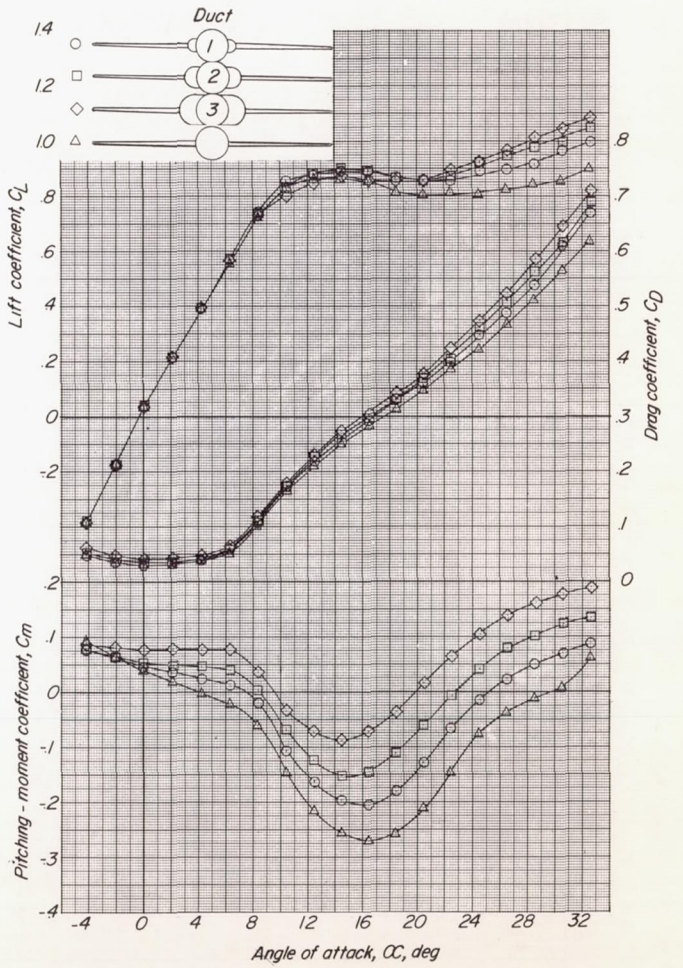

(d) Configuration FW_6VH_H.

Figure 6.- Concluded.

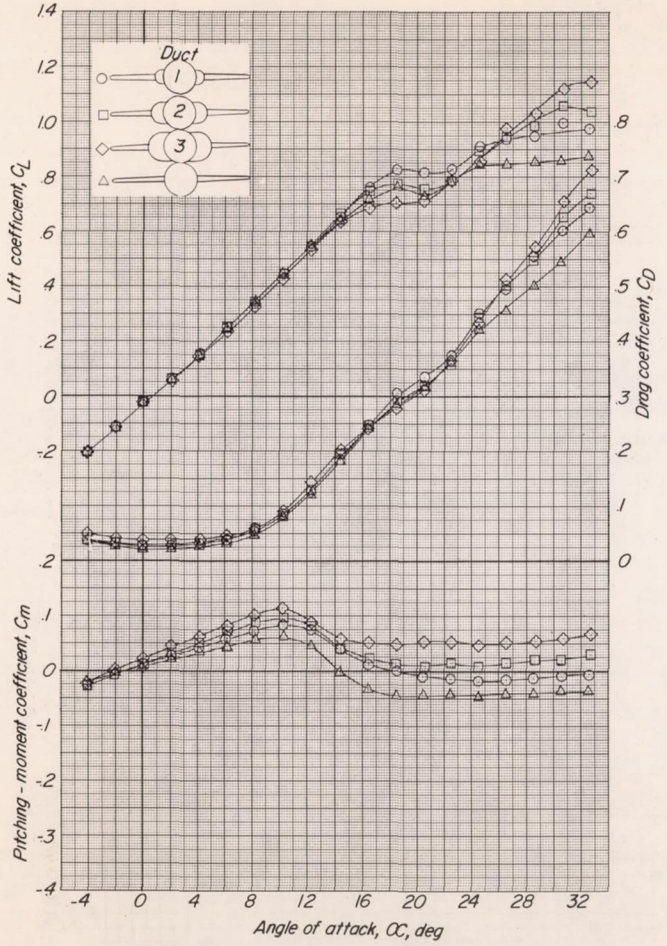

(a) Horizontal air ducts.

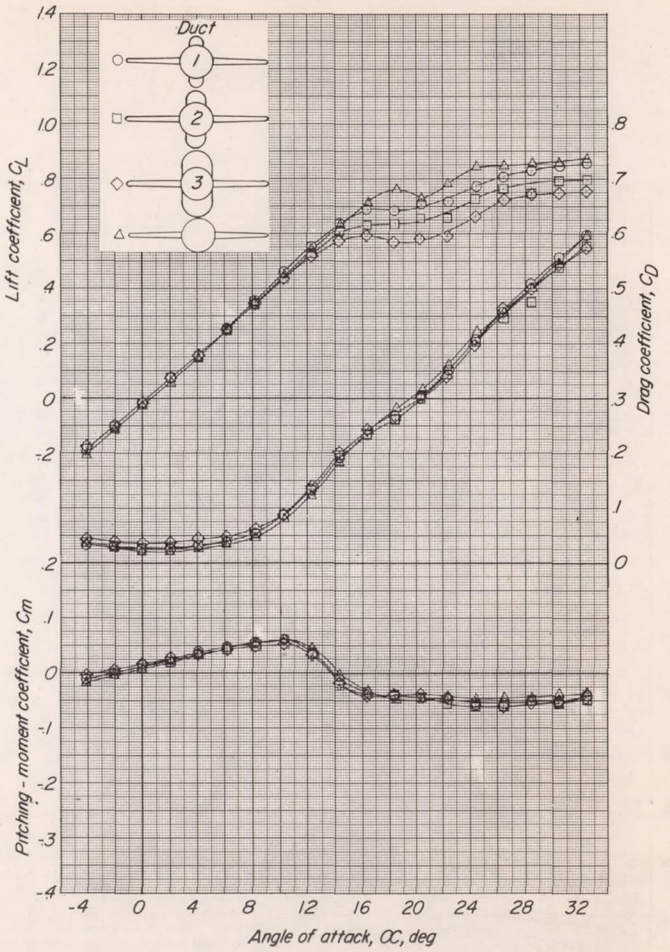

(b) Vertical air ducts.

Figure 7.- Effect of horizontal and vertical air ducts on the variation of C_L, C_D, and C_m with α for configuration FW_2.

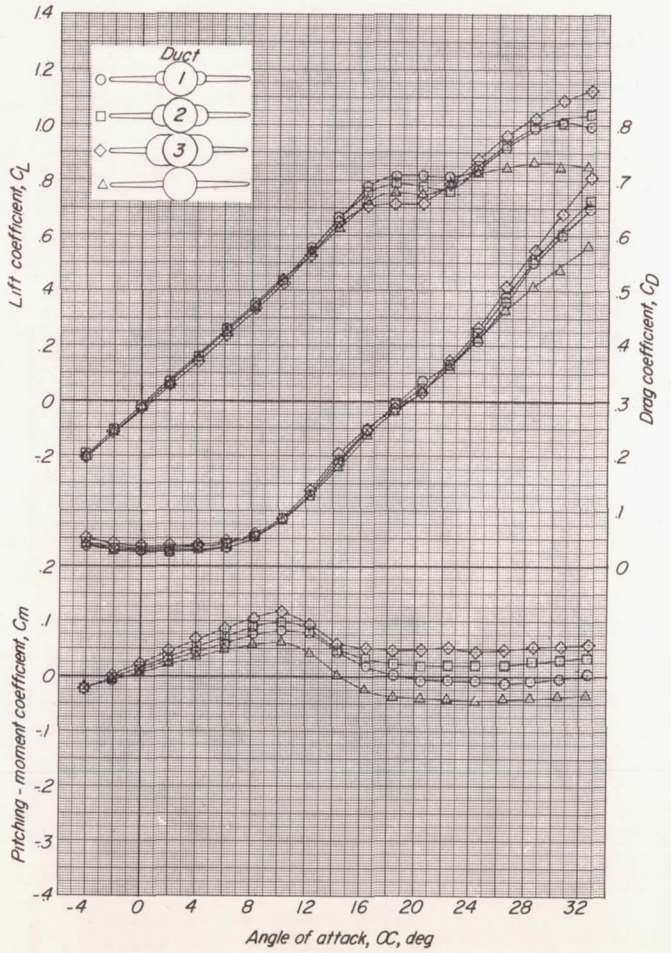

(a) Horizontal air ducts.

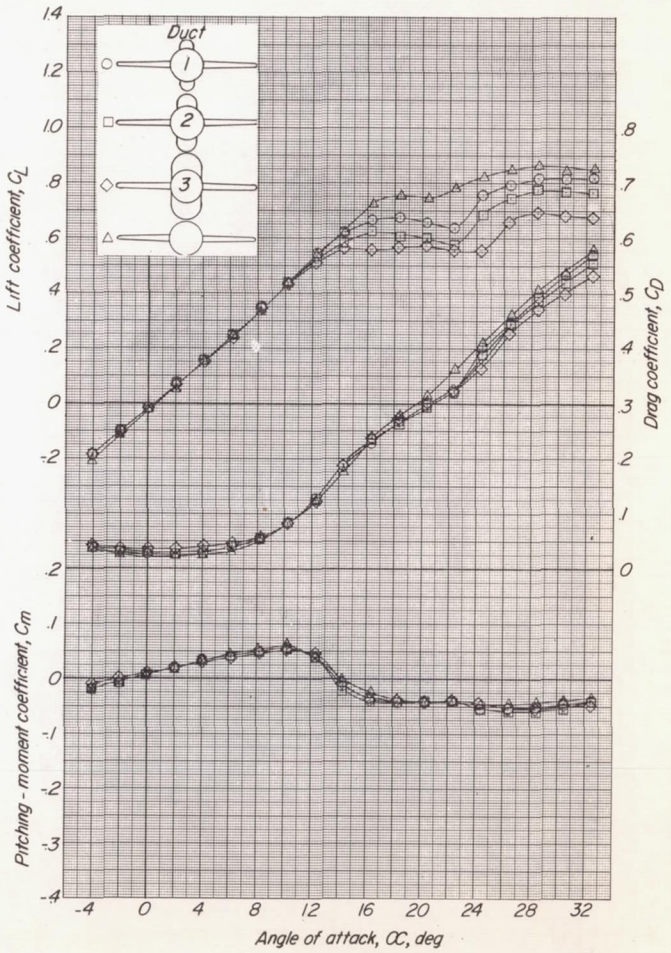

(b) Vertical air ducts.

Figure 8.- Effect of horizontal and vertical air ducts on the variation of C_L, C_D, and C_m with α for configuration FW_2V.

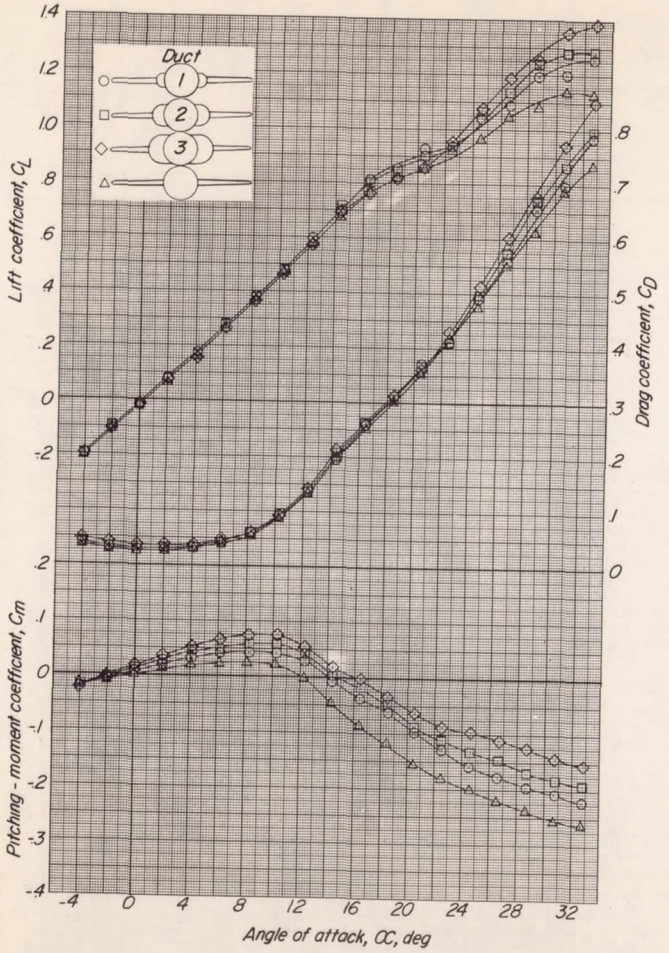

(a) Horizontal air ducts.

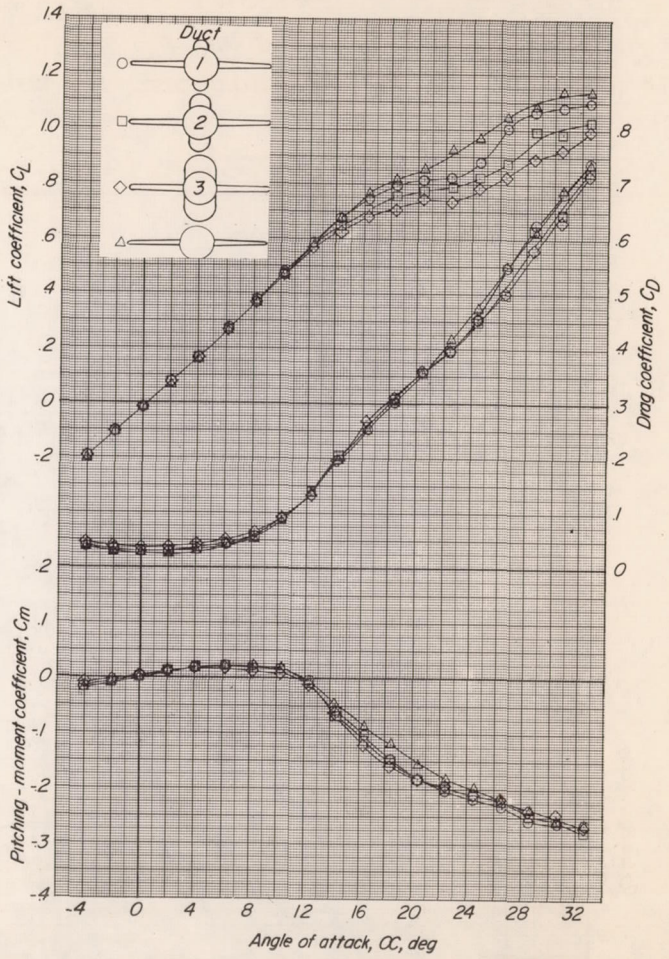

(b) Vertical air ducts.

Figure 9.- Effect of horizontal and vertical air ducts on the variation of C_L, C_D, and C_m with α for configuration FW_2VH_L.

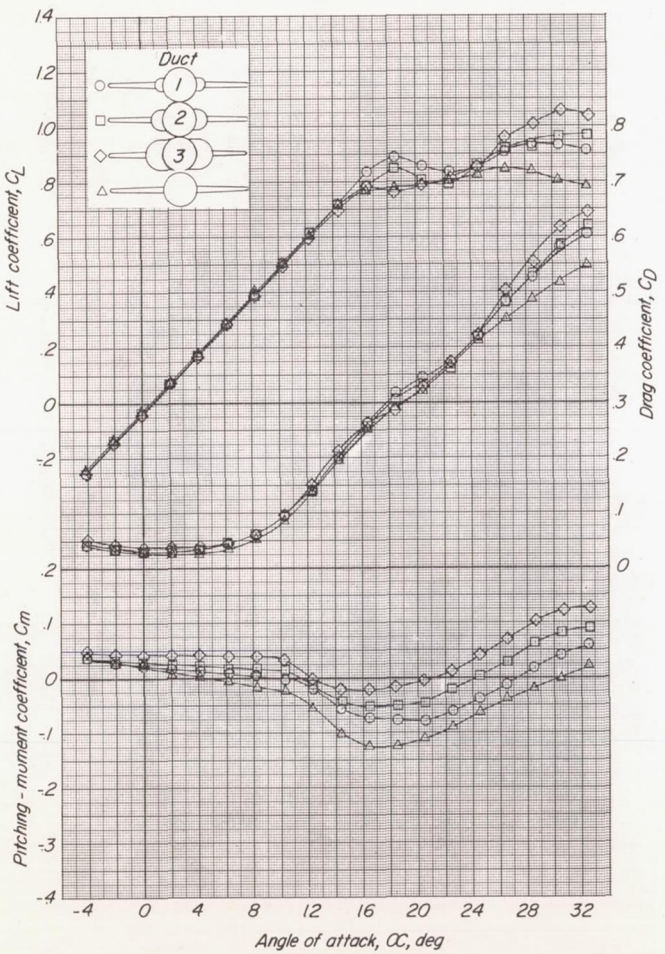

(a) Horizontal air ducts.

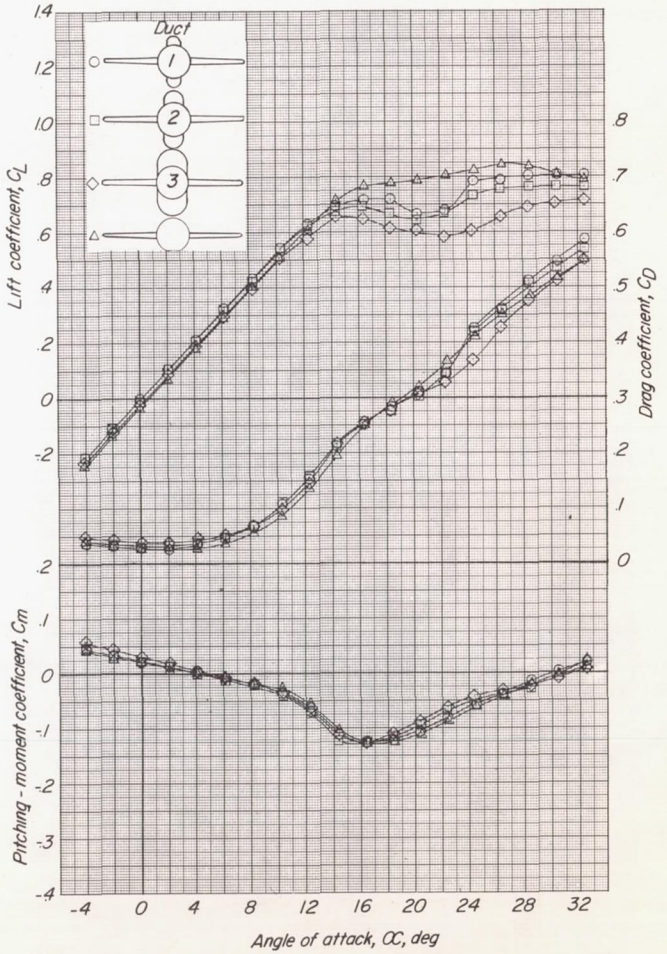

(b) Vertical air ducts.

Figure 10.- Effect of horizontal and vertical air ducts on the variation of C_L, C_D, and C_m with α for configuration FW_2VH_H.

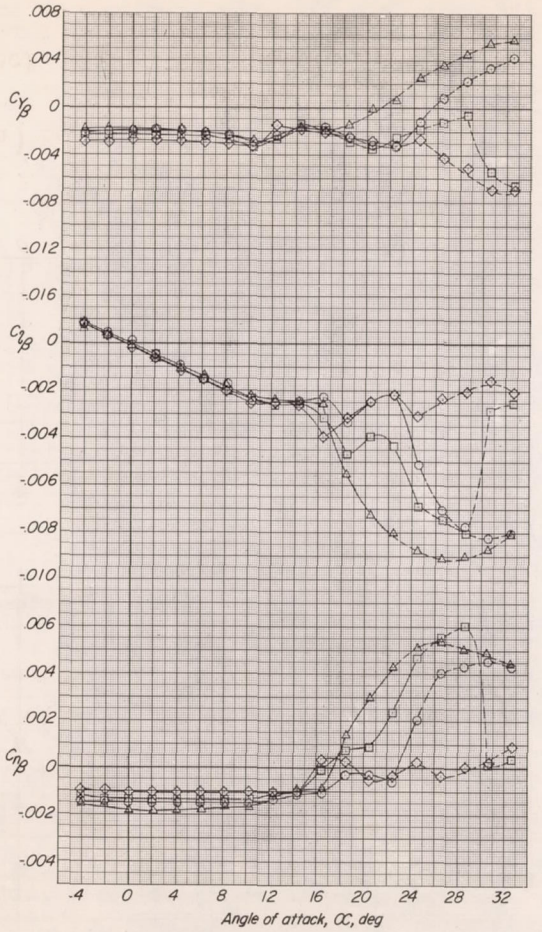

(a) Configuration FW_2.

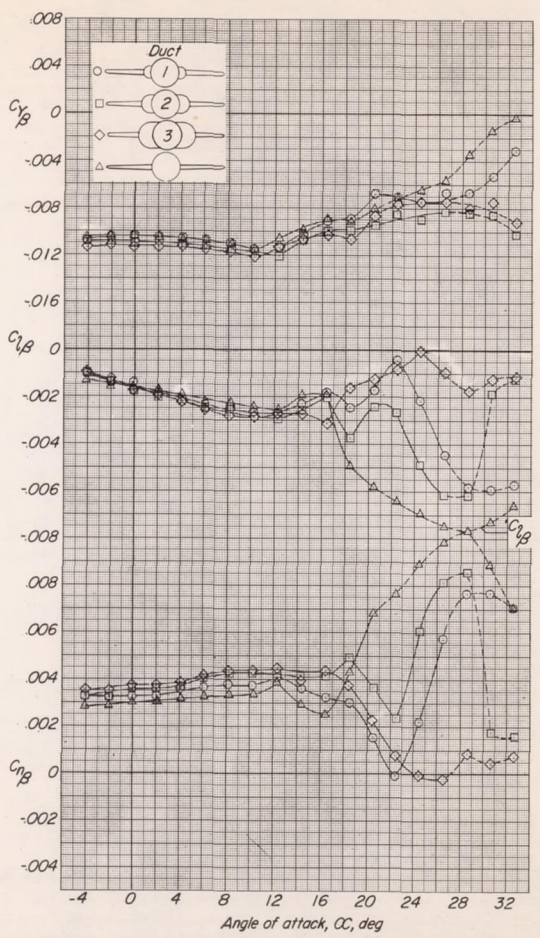

(b) Configuration FW_2V.

Figure 11.- Effect of horizontal air ducts on the variation of C_{Y_β}, C_{l_β}, and C_{n_β} with α for model arrangements having an unswept wing of aspect ratio 2.

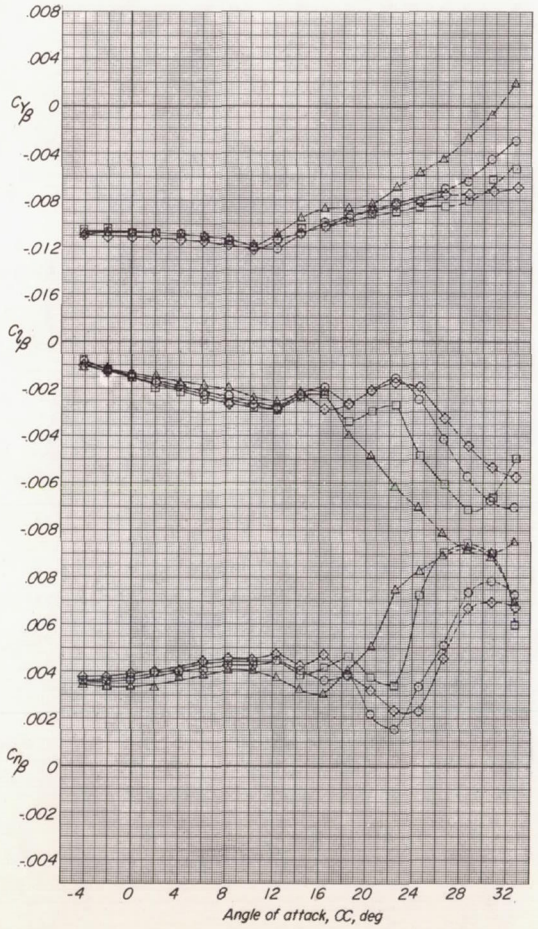

(c) Configuration FW_2VH_L.

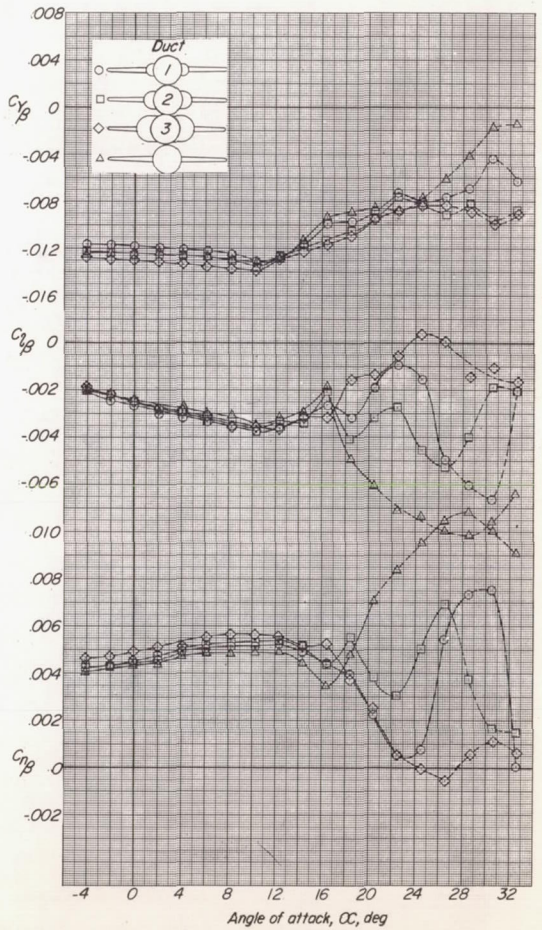

(d) Configuration FW_2VH_H.

Figure 11.- Concluded.

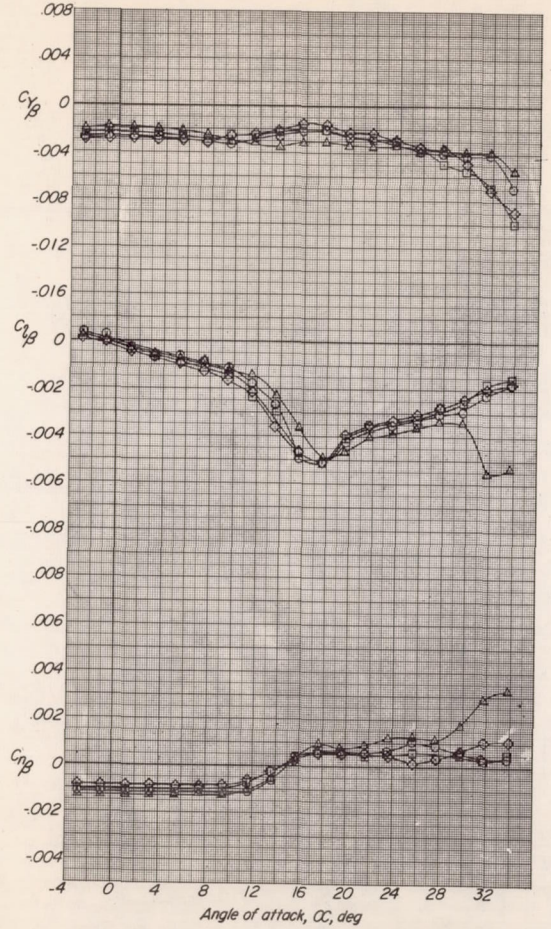

(a) Configuration FW_4.

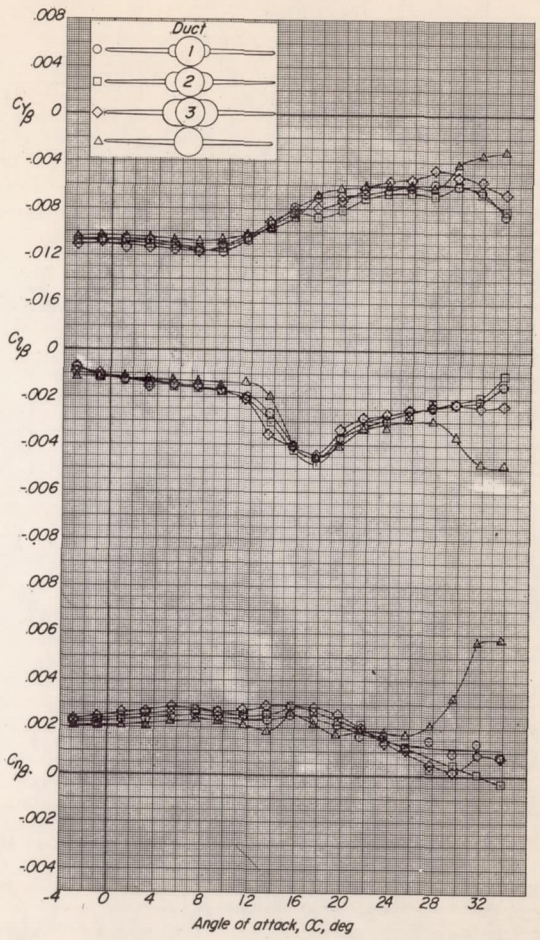

(b) Configuration FW_4V.

Figure 12.- Effect of horizontal air ducts on the variation of C_{Y_β}, C_{l_β}, and C_{n_β} with α for model arrangements having an unswept wing of aspect ratio 4.

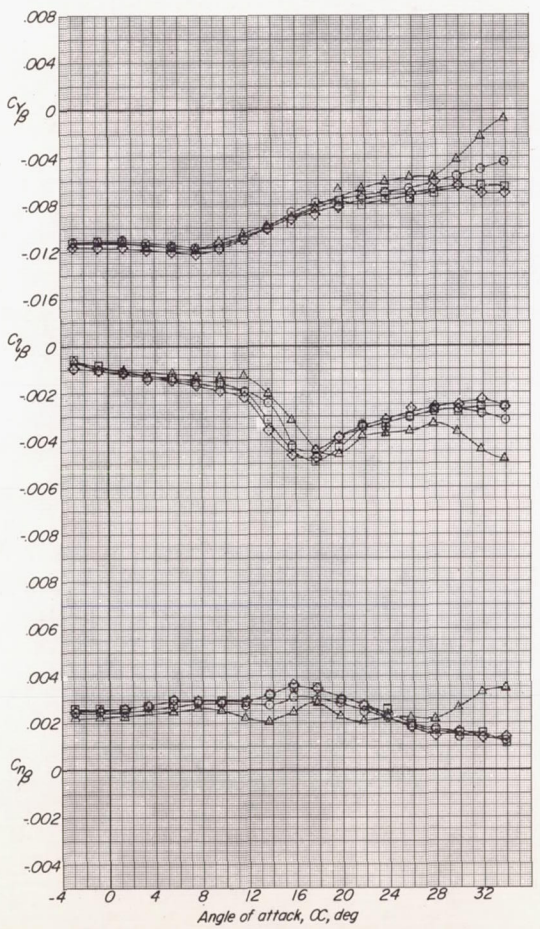

(c) Configuration FW_4VH_L.

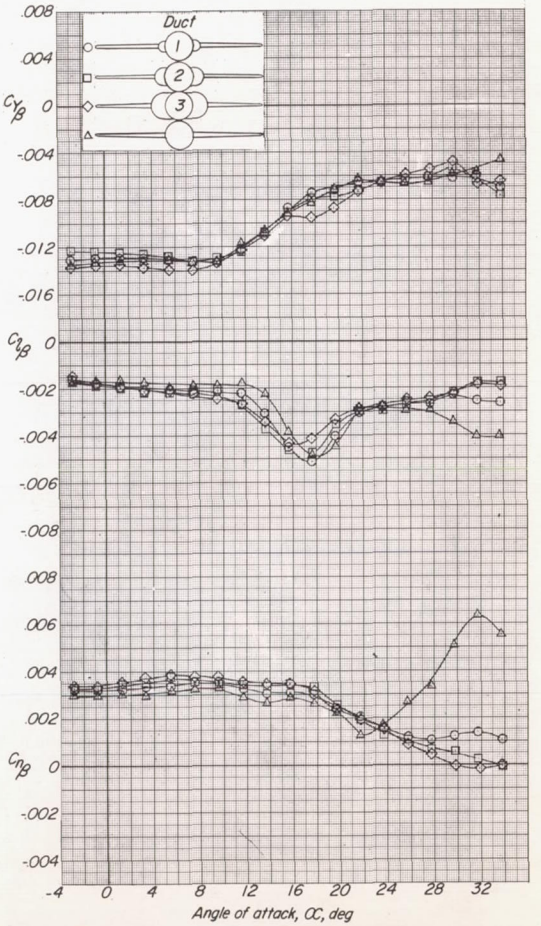

(d) Configuration FW_4VH_H.

Figure 12.- Concluded.

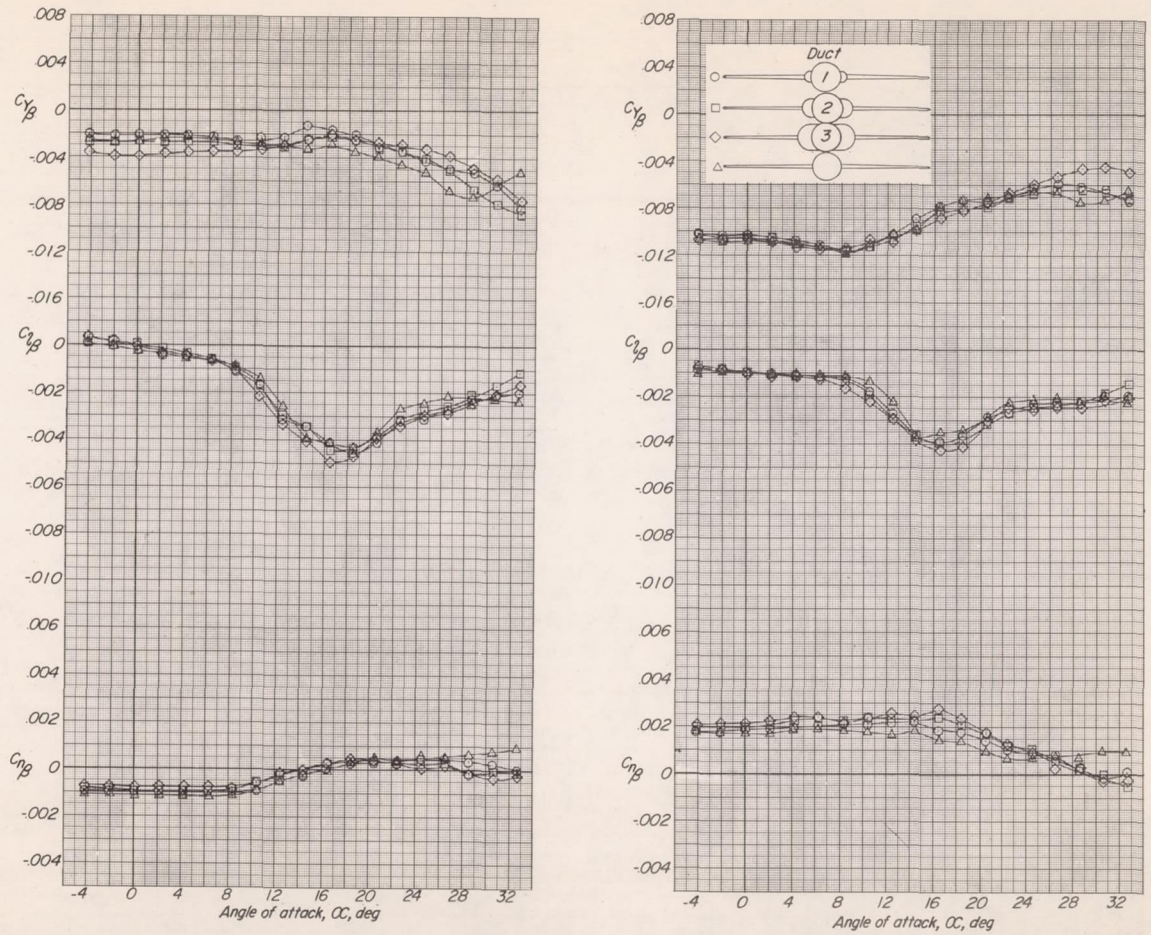

(a) Configuration FW6.

(b) Configuration FW6V.

Figure 13.- Effect of horizontal air ducts on the variation of C_{Y_β}, C_{l_β}, and C_{n_β} with α for model arrangements having an unswept wing of aspect ratio 6.

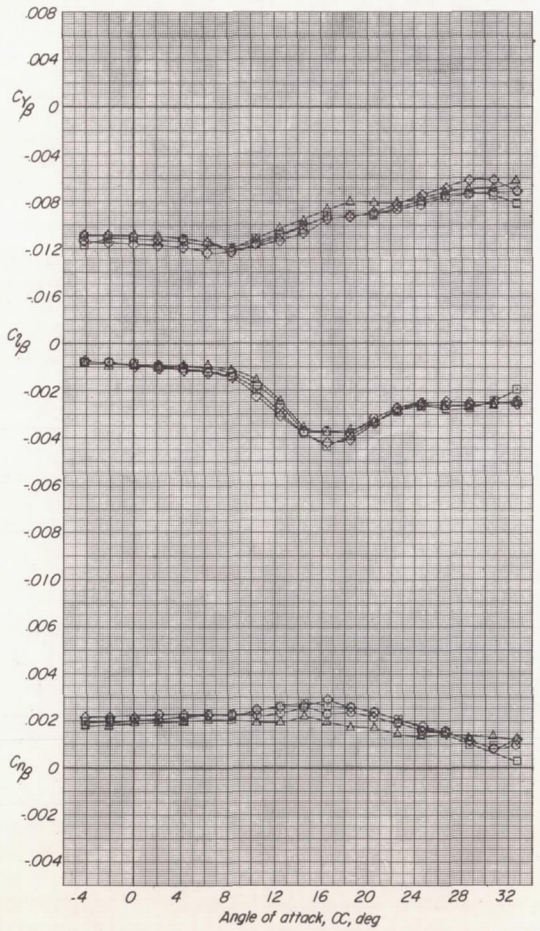

(c) Configuration FW_6VH_L.

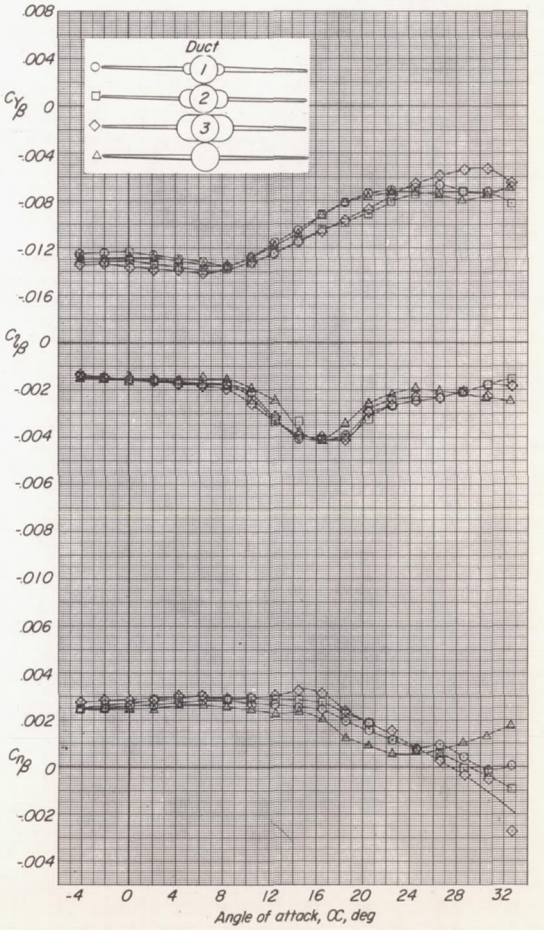

(d) Configuration FW_6VH_H.

Figure 13.- Concluded.

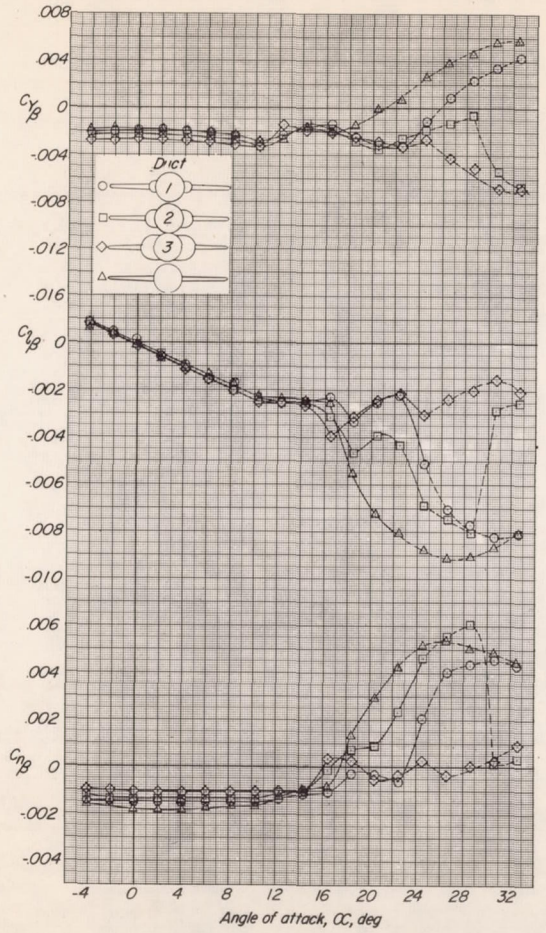

(a) Horizontal air ducts.

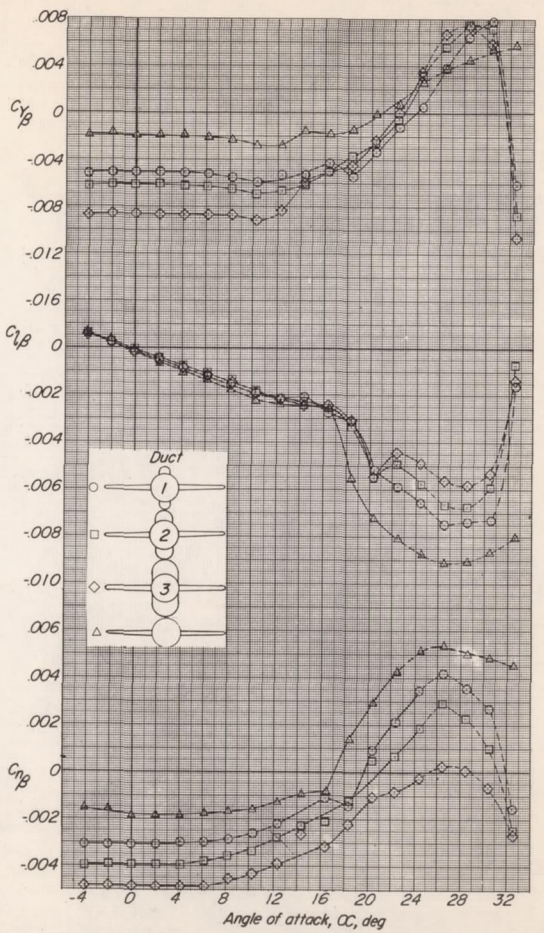

(b) Vertical air ducts.

Figure 14.- Effect of horizontal and vertical air ducts on the variation of C_{Y_β}, C_{l_β}, and C_{n_β} with α for configuration FW_2.

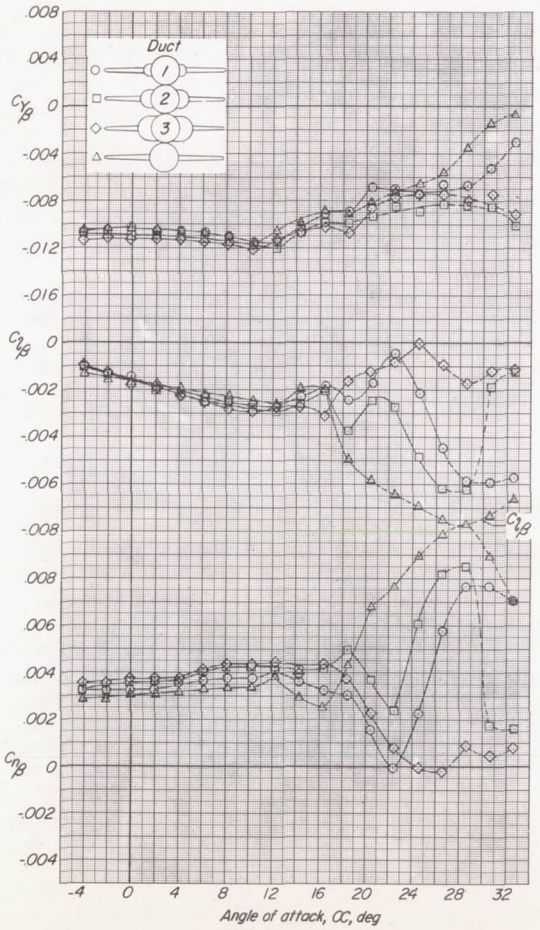

(a) Horizontal air ducts.

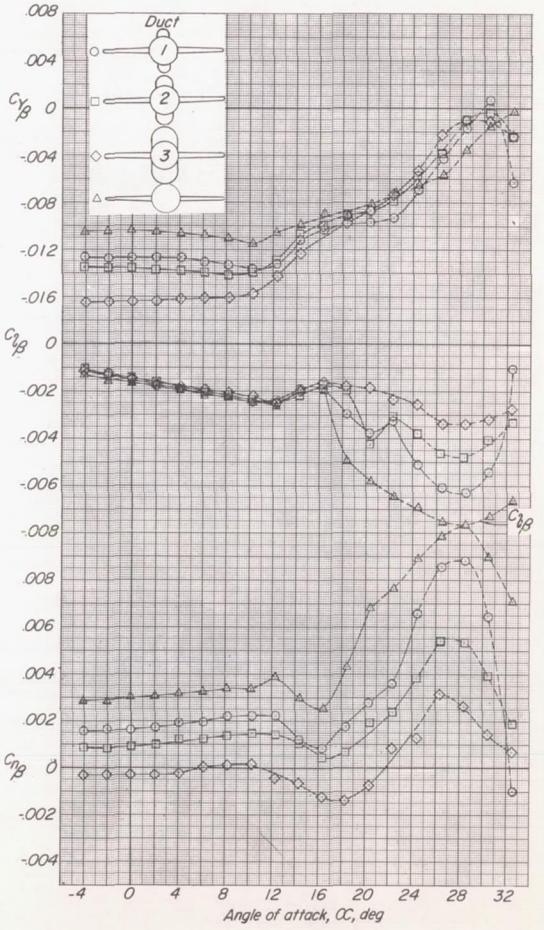

(b) Vertical air ducts.

Figure 15.- Effect of horizontal and vertical air ducts on the variation of C_{Y_β}, C_{l_β}, and C_{n_β} with α for configuration FW_2V.

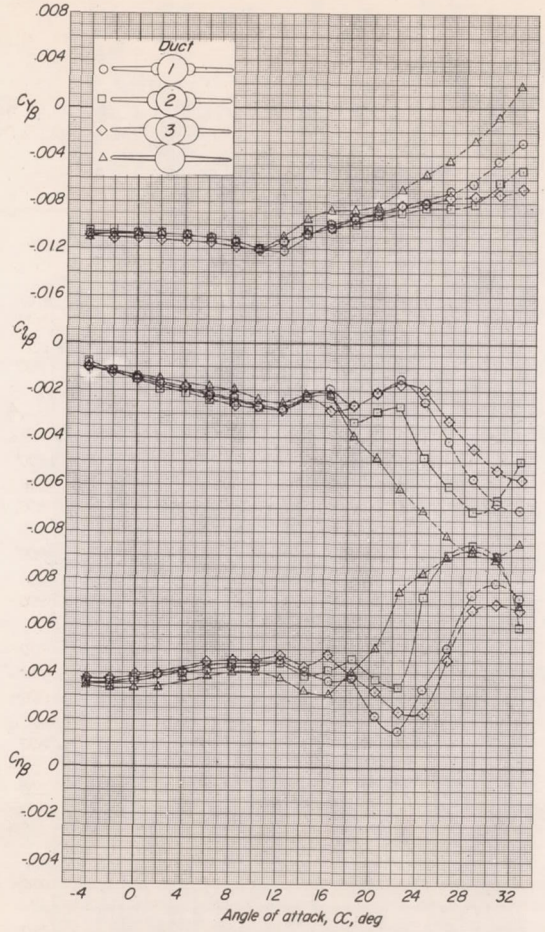

(a) Horizontal air ducts.

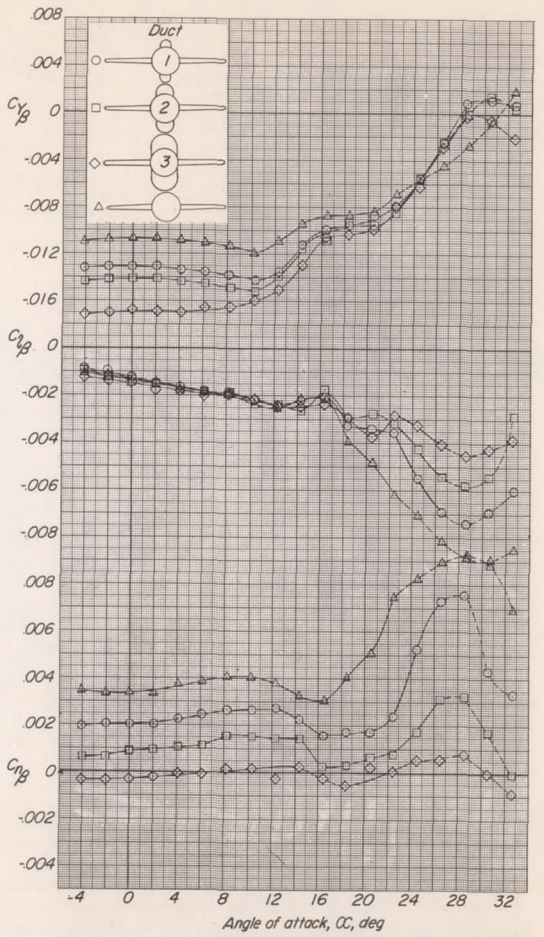

(b) Vertical air ducts.

Figure 16.- Effect of horizontal and vertical air ducts on the variation of C_{Y_β}, C_{l_β}, and C_{n_β} with α for configuration FW_2VH_L.

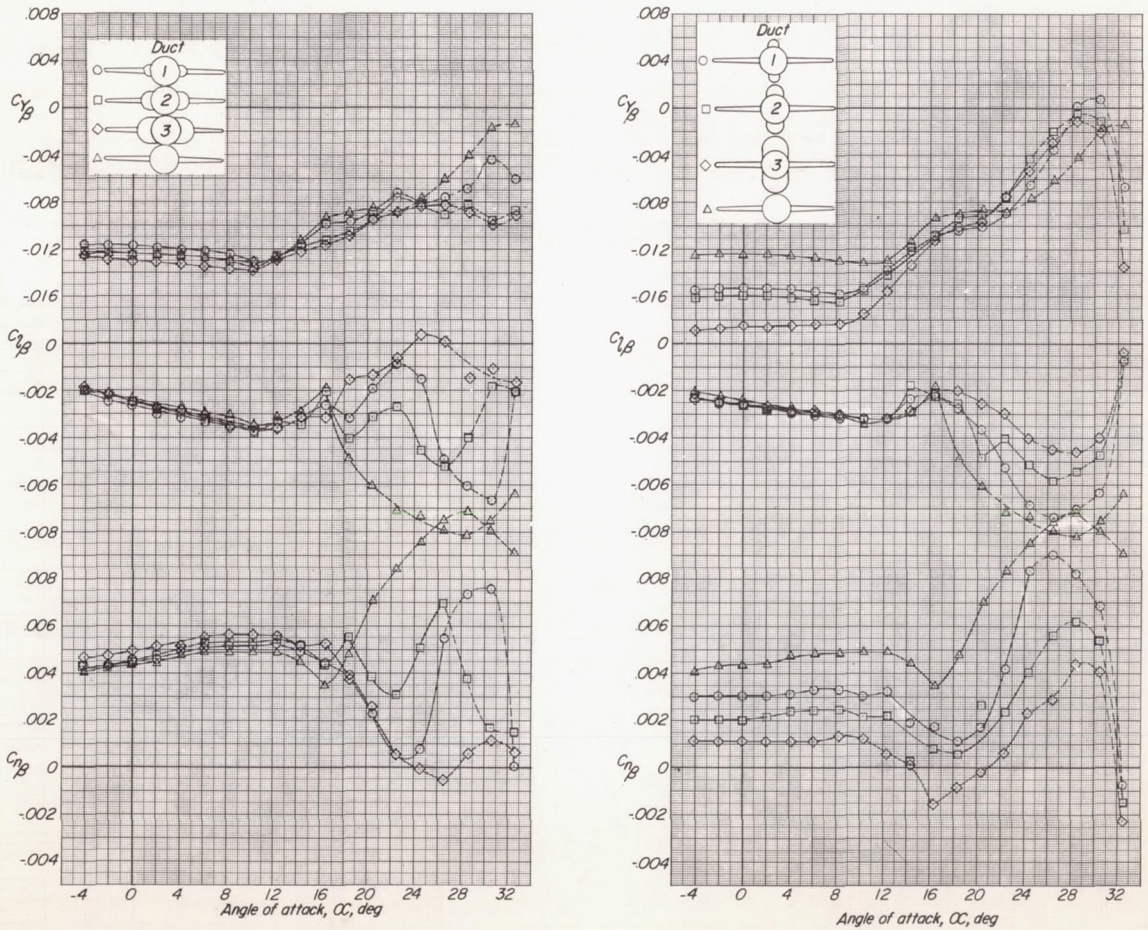

(a) Horizontal air ducts.

(b) Vertical air ducts.

Figure 17.- Effect of horizontal and vertical air ducts on the variation of C_{Y_β}, C_{l_β}, and C_{n_β} with α for configuration FW_2VH_H.

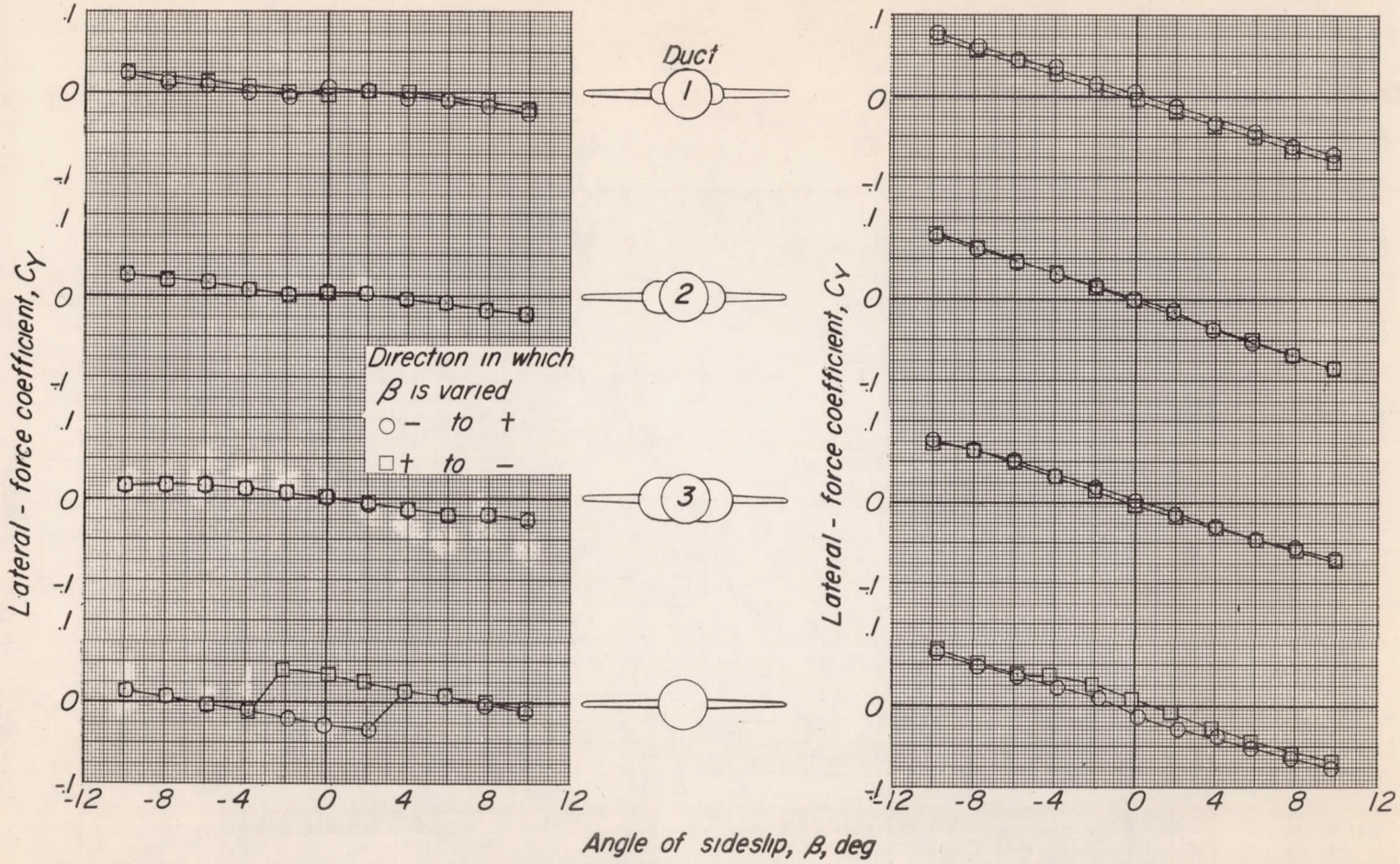

(a) Configuration FW_2.

(b) Configuration FW_2VH_H.

Figure 18.- Example of effect of aerodynamic hysteresis in the variation of C_Y with β for several representative model arrangements having an unswept wing of aspect ratio 2 and horizontal air ducts. $\alpha = 24.5^\circ$.

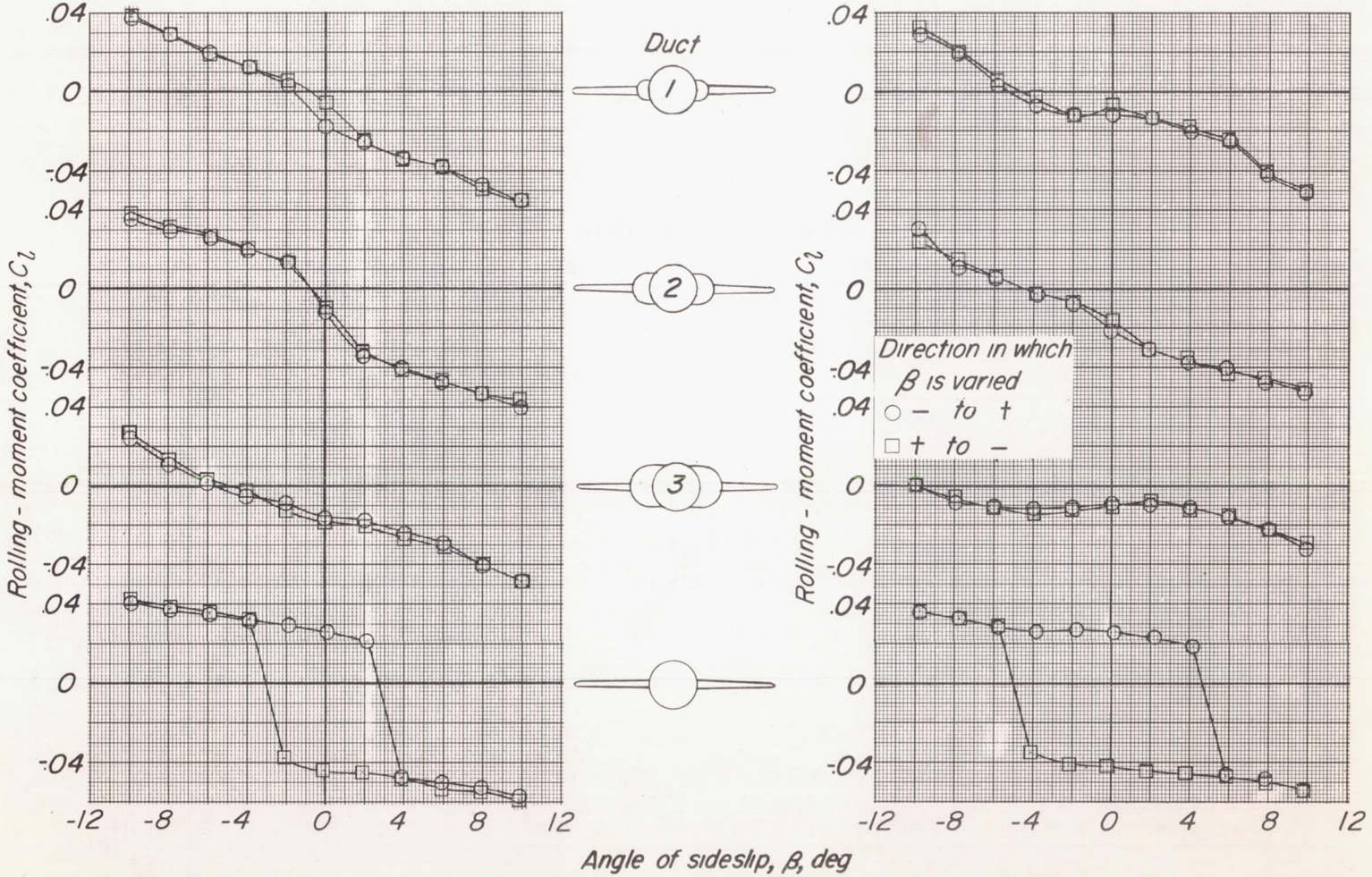

(a) Configuration FW_2.

(b) Configuration FW_2VH_H.

Figure 19.- Example of effect of aerodynamic hysteresis in the variation of C_l with β for several representative model arrangements having an unswept wing of aspect ratio 2 and horizontal air ducts. $\alpha = 24.5^\circ$.

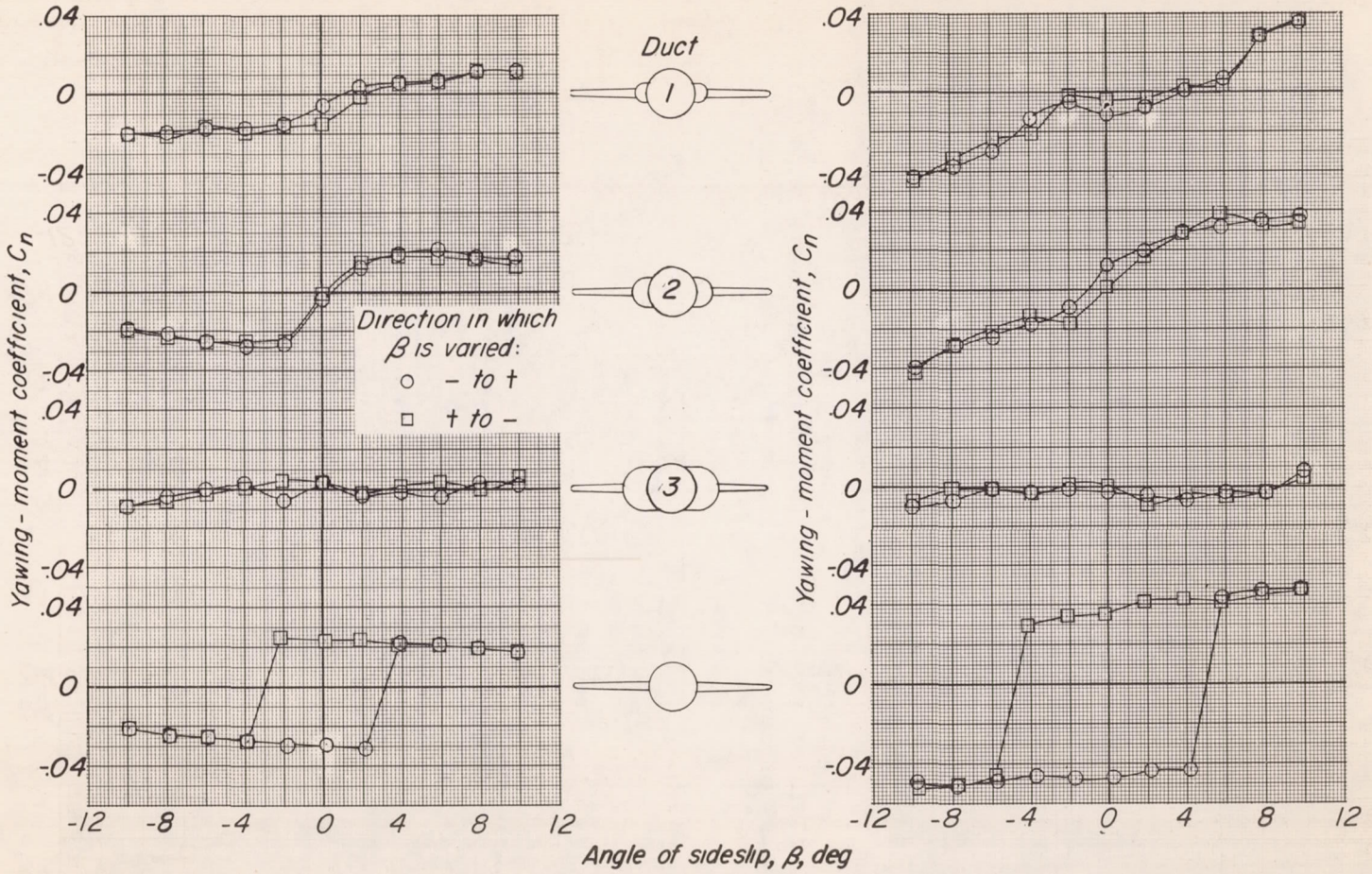

(a) Configuration FW_2.

(b) Configuration FW_2VH_H.

Figure 20.- Example of effect of aerodynamic hysteresis in the variation of C_n with β for several representative model arrangements having an unswept wing of aspect ratio 2 and horizontal air ducts. $\alpha = 24.5^\circ$.

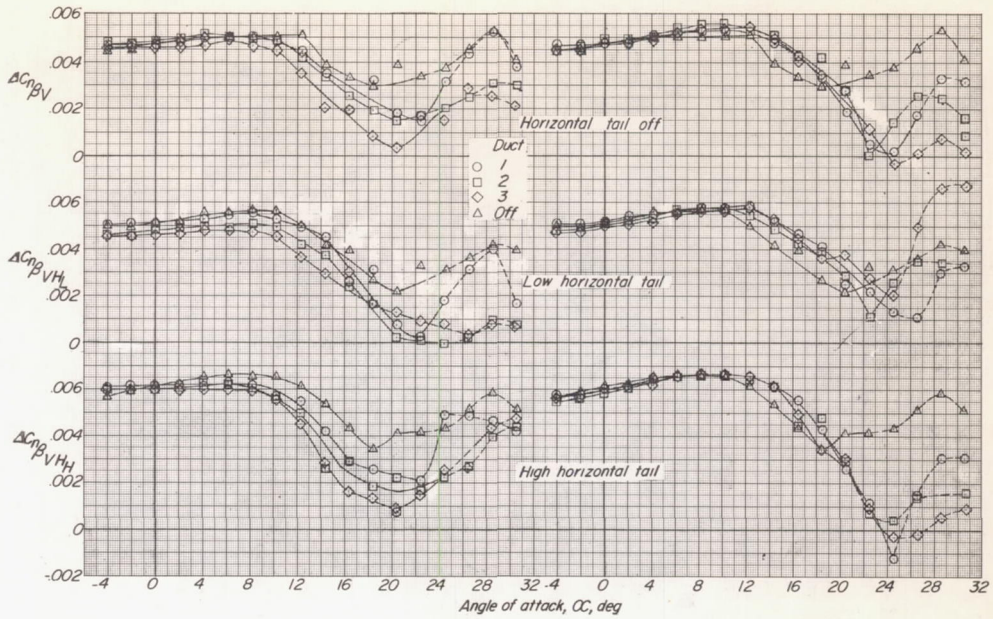

(a) Vertical ducts on models having a wing of aspect ratio 2.

(b) Horizontal ducts on models having a wing of aspect ratio 2.

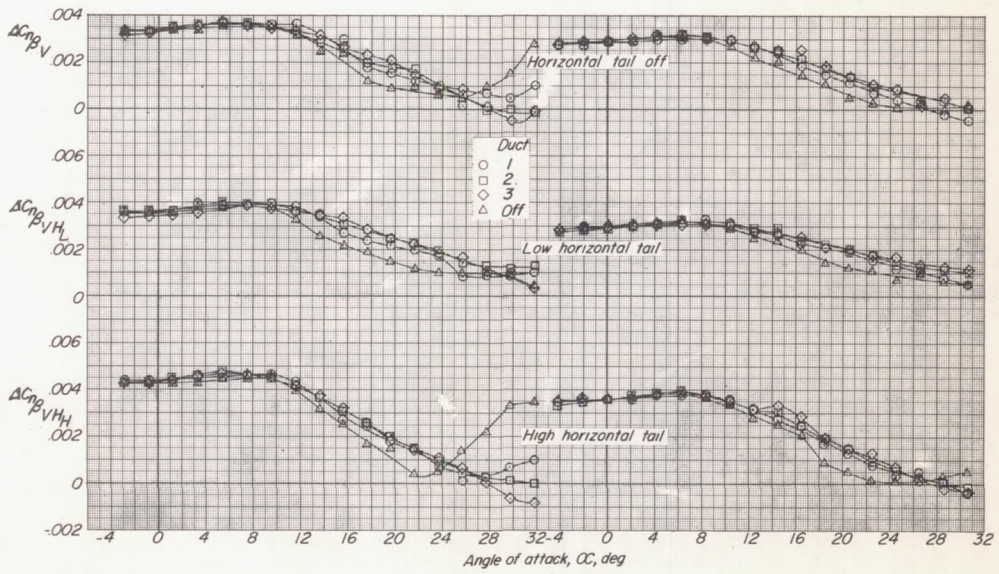

(c) Horizontal ducts on models having a wing of aspect ratio 4.

(d) Horizontal ducts on models having a wing of aspect ratio 6.

Figure 21.- Effect of ducts on the contribution of various tail assemblies to the directional stability of several unswept wing models.

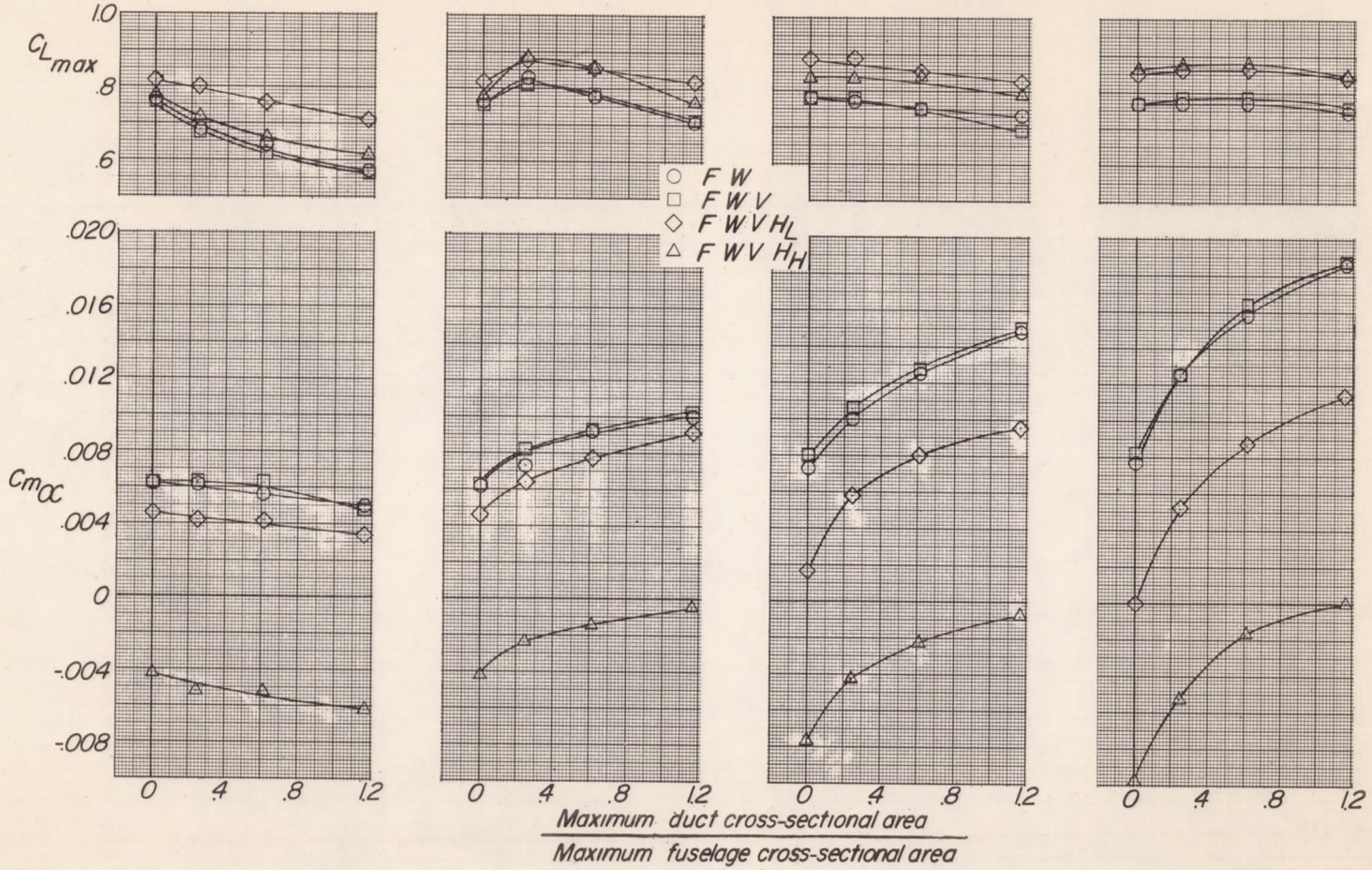

(a) Vertical ducts on models having a wing of aspect ratio 2.

(b) Horizontal ducts on models having a wing of aspect ratio 2.

(c) Horizontal ducts on models having a wing of aspect ratio 4.

(d) Horizontal ducts on models having a wing of aspect ratio 6.

Figure 22.- Summary of effects of air ducts on the longitudinal characteristics of unswept-wing models. Slopes measured at $\alpha = 0^{\circ}$.

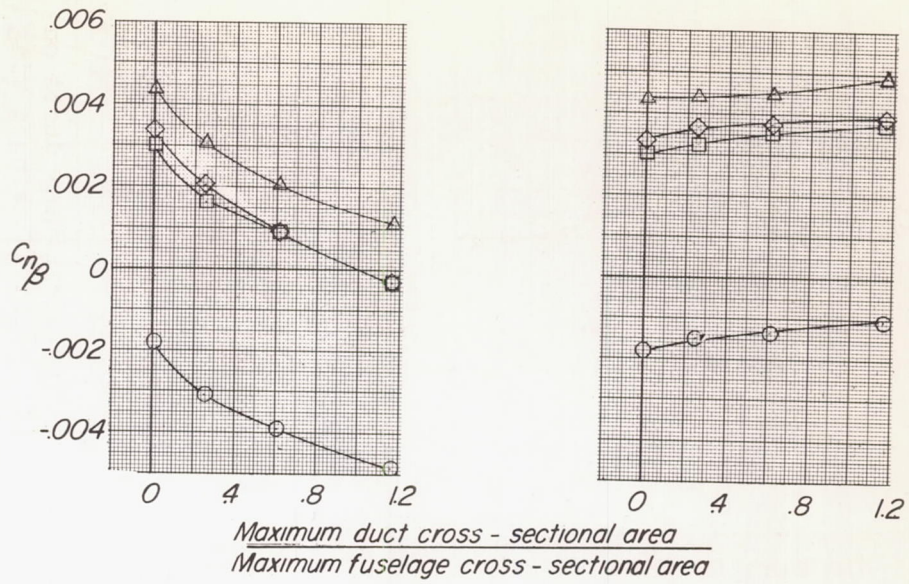

(a) Vertical ducts on models having a wing of aspect ratio 2.

(b) Horizontal ducts on models having a wing of aspect ratio 2.

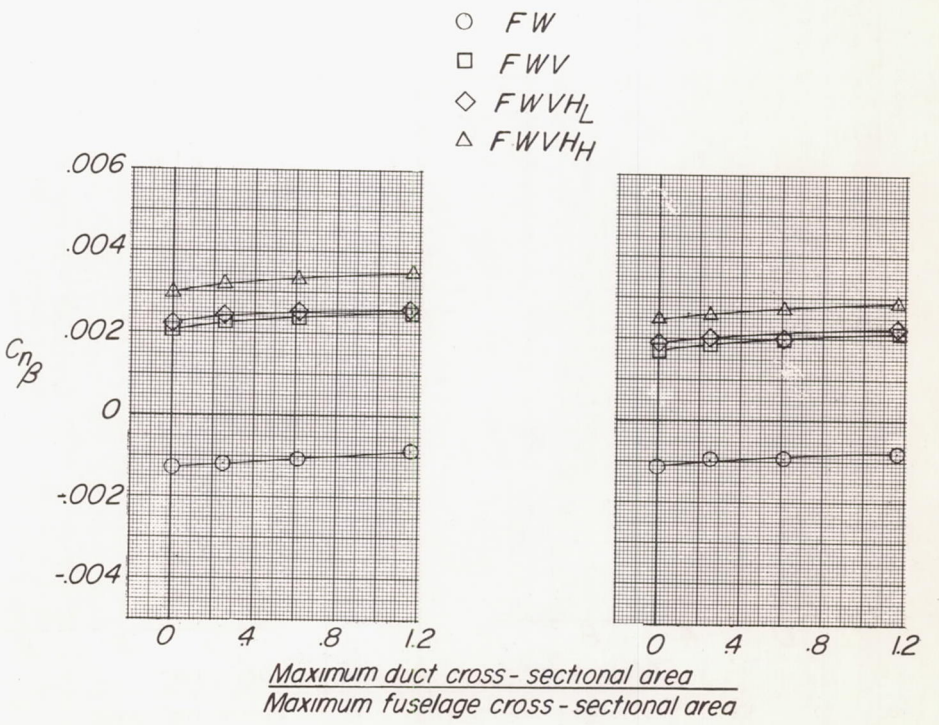

(c) Horizontal ducts on models having a wing of aspect ratio 4.

(d) Horizontal ducts on models having a wing of aspect ratio 6.

Figure 23.- Summary of effects of air ducts on the directional stability characteristics of unswept-wing models. $\alpha = 0^\circ$.

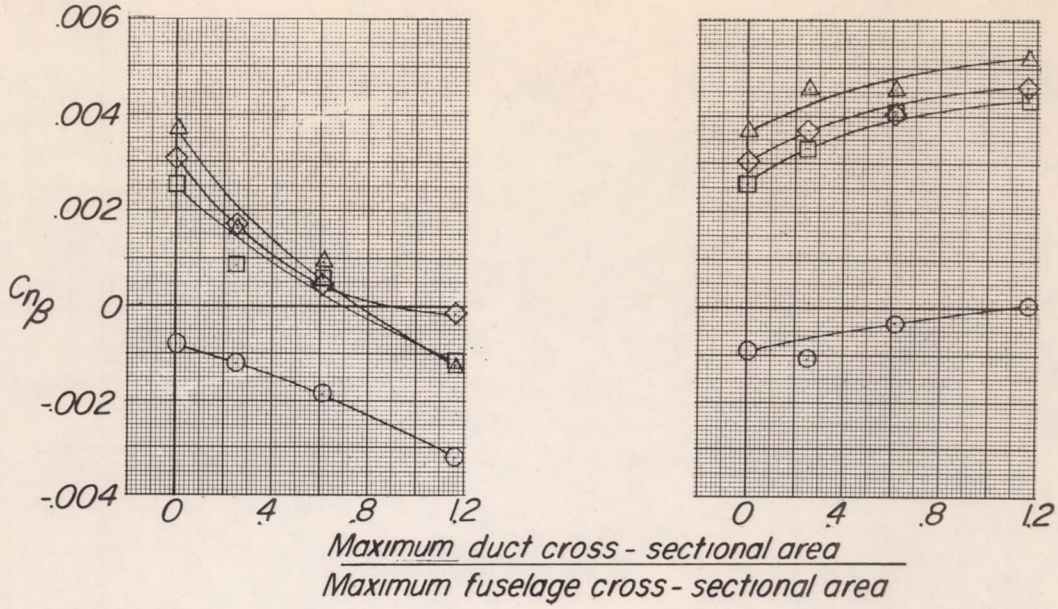

(a) Vertical ducts on models having a wing of aspect ratio 2.

(b) Horizontal ducts on models having a wing of aspect ratio 2.

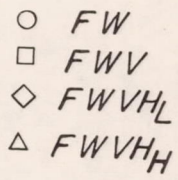

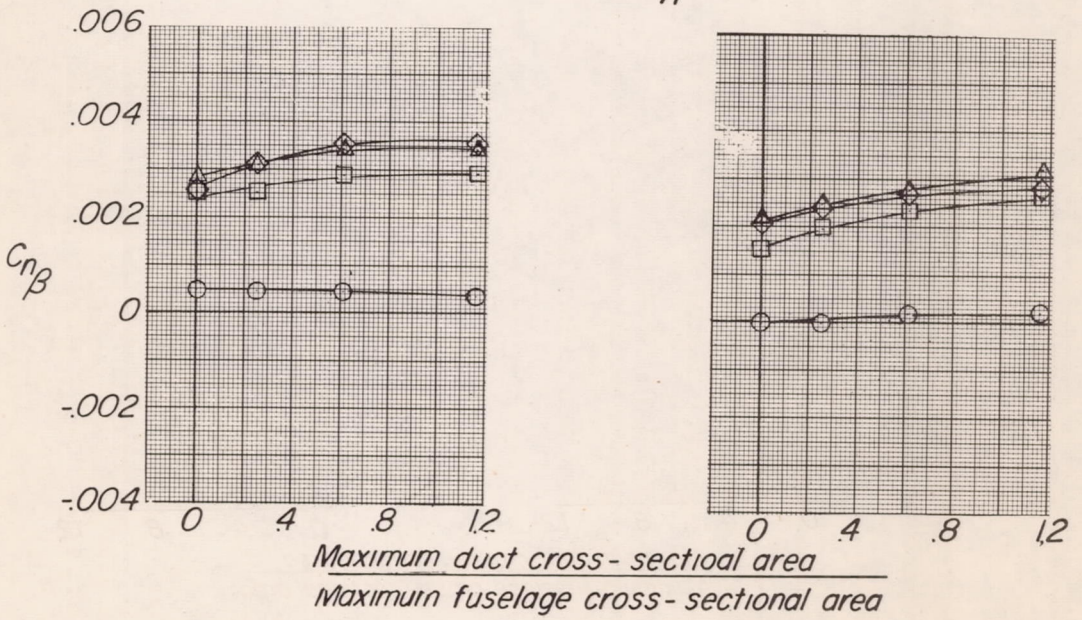

(c) Horizontal ducts on models having a wing of aspect ratio 4.

(d) Horizontal ducts on models having a wing of aspect ratio 6.

Figure 24.- Summary of effects of air ducts on the directional stability characteristics of unswept-wing models. $\alpha = 16^\circ$.